Cooperative Constrained Enclosing Control of Multirobot Systems in Obstacle Environments

Ke Lu, Shi-Lu Dai, Member, IEEE, and Xu Jin, Member, IEEE

Abstract—This paper develops a novel cooperative constrained control framework to solve the moving-target enclosing problem for multirobot systems, where safe navigation and formation precision are concerned in obstacle environments. When moving obstacles block the encircling motion, the enclosing formation contracts towards the target with a precise spacing pattern. Without a priori knowledge of environment information, the mobile robot group can track and enclose a moving target while guaranteeing limited sensing requirements and collision avoidance with the target, neighbouring robots, and obstacles. Under the precision constraint, with an encircling speed assigned to only one robot, the mobile robots are driven by their neighbours until all robots enclose the target as a whole. With the help of velocity observers, the robot group can converge to a small neighborhood of the desired enclosing formation without knowing the target's velocity. Simulation results demonstrate the effectiveness of the proposed constrained control strategy.

Index Terms—Target enclosing, barrier function, limited sensing, collision avoidance, obstacle avoidance.

I. INTRODUCTION

Over the last few decades, cooperative control of multiagent systems has received considerable attention [1]–[4]. In particular, the objective of enclosing control is to attain a formation orbiting around a target for entrapment, protection, or surveillance. This enclosing formation can block the way to a specific surrounded area, and also can simultaneously provide different perspectives of a target. For example, when the information of interest is a general view of a monitoring target/area rather than a single view of one sensor, sensor data

The work of Ke Lu and Shi-Lu Dai was supported in part by the National Natural Science Foundation of China under Grant 42227901, Grant 61973129, Grant 62273156, and Grant 62073090, in part by the Guangdong Basic and Applied Basic Research Foundation under Grant 2021A1515012004, and in part by the Innovation Group Project of Southern Marine Science and Engineering Guangdong Laboratory (Zhuhai) (No. SML2022008). The work of Xu Jin was supported in part by the United States National Science Foundation under Grant 2131802. (Corresponding author: Shi-Lu Dai.)

Ke Lu is with the School of Automation Science and Engineering, South China University of Technology, Guangzhou 510641, China (e-mail: lukenanlin@163.com).

Shi-Lu Dai is with the School of Automation Science and Engineering, Key Laboratory of Autonomous Systems and Networked Control of Ministry of Education, South China University of Technology, Guangzhou 510641, China, and also with the Southern Marine Science and Engineering Guangdong Laboratory (Zhuhai), Zhuhai 519000, China (e-mail: audaisl@scut.edu.cn).

Xu Jin is with the Department of Mechanical and Aerospace Engineering, University of Kentucky, Lexington, KY 40506 USA (e-mail: xu.jin@uky.edu).

from all vehicles cooperatively monitoring a ground target/area is fused to provide comprehensive information or a view of the entire field. This problem has been widely studied in [5]–[10], where a stationary or moving target is enclosed by a group of autonomous agents. Tracking and encircling a moving target becomes more challenging when the target's velocity is not available for the control algorithm. For the case where the position or velocity of a target is unknown, observers are typically constructed for multiagent systems to estimate the unknown information [11], [12]. In terms of the enclosing formation, multiple agents are driven to surround a target with *even* distribution in [13], [14]. However, in some applications, an even distribution might not be preferred, and in contrast, the convergence to any prescribed spacing formation along the circle might provide a better performance [15]–[18].

On the one hand, coordination control design is usually concerned with the safety problem, which requires that collisions with neighbouring agents or/and obstacles never occur. On the other hand, an onboard sensor can only work reliably within a certain range due to its limited sensing capability, which is another safety hazard. In [19], [20], the problems of collision avoidance and connectivity maintenance for multiagent systems are addressed by handling inter-agent distance constraints. In the context of enclosing control, the inter-agent collision avoidance is taken into account to enhance the target enclosing performance in [21], [22]. Although some works have addressed the problem of collision avoidance with either the target or neighbours, the obstacle avoidance is also of great importance for enclosing control design since the operating environment is often severe and cluttered. In such an obstacle-cluttered environment, an elastic formation is preferred [23], where multiagent systems generate a timevarying formation to avoid the obstacle, but the environment information is required to be known a priori.

Constrained control design can ensure the system output to remain within a certain range specified by safety requirements. This constrained control problem has been extensively studied, e.g., [24]–[26], where different kinds of barrier functions are developed for constrained control systems. Due to the advantage in handling constrained systems, barrier functions have been employed to guarantee the collision avoidance or/and limited sensing capabilities for multiagent systems [27]–[32]. In addition, potential functions [33]–[37] can be integrated into control Lyanpunov synthesis to drive autonomous agents convergence to a desired formation without any collision with obstacles. Even though the safety problem has been partially addressed in the aforementioned works, the moving-target

enclosing control problem with the concern of safety and precision constraints is still a challenging issue. On the one hand, the enclosing control design is required to simultaneously meet constraint requirements from the target, neighbouring agents, and obstacles during the encircling motion. On the other hand, due to the higher priority of obstacle avoidance, formation errors sometimes are inevitably required to deviate from the origin, which implies the formation precision against safety. Consequently, the constraints with different types arise in the moving-target enclosing control design. A loose interagent constraint implies formation error tolerance, allowing the enclosing formation to be elastic for obstacle avoidance without violating any constraint. In contrast, a tight inter-agent constraint can force the multiagent systems to converge to a precise formation. Furthermore, the target-agent distance and the spacing among neighbouring agents cannot be too small or too large, which implies the two side constraints. In contrast, the relative distance to the obstacles cannot be too small only, which means the one side constraint. Hence, the aforementioned control algorithms cannot be directly extended to the enclosing formation control design in obstacle environments. How to develop a constrained control framework without the knowledge of target's velocity is an important research topic yet to be examined.

In this work, we develop a novel cooperative constrained control framework to solve the moving-target enclosing problem for a group of nonholonomic mobile robots in obstacle environments. The novelty of the work lies on the constrained control framework where the constraints from both safety navigation and formation precision are considered such that (i) the limited sensing requirements and collision avoidance with the target, neighbouring robots, and obstacles are guaranteed despite the lack of target's velocity; and (ii) while only one robot is assigned an encircling speed, the robot group can converge to a small neighbourhood of the desired formation, enclosing a moving target. Different from [12]-[15] where an even spacing formation is generated, or a desired spacing pattern is obtained by adjusting robot's velocity or position, the formation precision constraint studied in this work forces the robots to generate a desired spacing formation and revolve around a moving target. Compared with the works [5], [22] that prevent collisions with either the target or neighbouring robots, the presented algorithm further considers the limited sensing constraint and collision avoidance with moving obstacles. The contributions of this work are summarized as follows.

- (i) A novel cooperative constrained control strategy is proposed to address the moving-target enclosing problem, where both safety navigation and formation precision are considered, despite the lack of target's velocity.
- (ii) The safety constraints, which considers the limited sensing capability of onboard sensors, and target-robot/interrobot collision avoidance, allow for the embedded potential function deforming the enclosing formation for obstacle avoidance.
- (iii) The presented algorithm enables mobile robots to avoid collision with the nearest static or moving obstacle without a priori knowledge of environment information, and

- the local minima problem resulted from potential functions is prevented with the target's trajectory sufficiently far from obstacles.
- (iv) With an encircling speed assigned to only one robot, the precision constraint drives the robot group to converge to a desired spacing formation and enclose a moving target.

II. PROBLEM FORMULATION

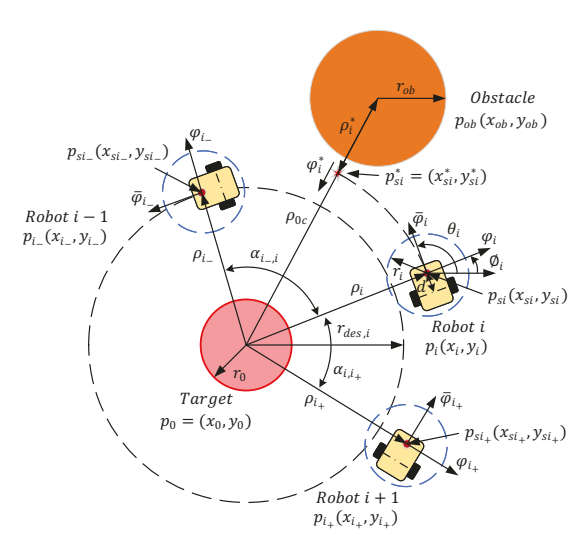


Fig. 1. Illustration of enclosing a target by multiple mobile robots in an obstacle environment.

Consider a moving target is enclosed by a group of $n \geq 2$ nonholonomic mobile robots in a plane. Let the index set $\mathcal{N} = \{1,...,n\}$. The kinematics of robot $i, i \in \mathcal{N}$, is modeled as

$$\dot{p}_i(t) = \begin{bmatrix} \cos \theta_i(t) \\ \sin \theta_i(t) \end{bmatrix} v_i(t)$$

$$\dot{\theta}_i(t) = \omega_i(t)$$
(1)

where $p_i(t) = [x_i(t) \ y_i(t)]^T \in \mathbb{R}^2$ is the position of robot i with respect to a global coordinate frame, $\theta_i(t)$ is its heading angle, $v_i(t)$ and $\omega_i(t)$ are the linear and angular velocity control inputs, respectively. As shown in Fig. 1, the onboard sensor of robot i is installed at the position $p_{si}(t) = [x_{si}(t) \ y_{si}(t)]^T$ which is shifted a non-zero distance d from $p_i(t)$ along direction $\theta_i(t)$. The position $p_{si}(t)$ is described by $p_{si}(t) = p_i(t) + d[\cos\theta_i(t) \sin\theta_i(t)]^T$ whose dynamics is modeled as

$$\dot{p}_{si}(t) = H_i(t)u_i(t) \tag{2}$$

where $u_i(t) = [v_i(t) \ \omega_i(t)]^T$ and $H_i(t)$ is defined as

$$H_i(t) = \begin{bmatrix} \cos \theta_i(t) & -d \sin \theta_i(t) \\ \sin \theta_i(t) & d \cos \theta_i(t) \end{bmatrix}.$$
 (3)

It should be noted that $det(H_i(t)) = d$ implies $H_i(t)$ is invertible with $d \neq 0$. The moving target is governed by

$$\dot{p}_0(t) = v_0(t)$$

where $p_0(t) = [x_0(t) \ y_0(t)]^T \in \mathbb{R}^2$ and $v_0(t) \in \mathbb{R}^2$ are the position and velocity of the target, respectively. The relative

distance between the onboard sensor of robot i and the moving target is defined as

$$\rho_i(t) = \sqrt{(x_{si}(t) - x_0(t))^2 + (y_{si}(t) - y_0(t))^2}$$
 (4)

whose derivative yields

$$\dot{\rho}_i(t) = \varphi_i^T(t)[\dot{p}_{si}(t) - v_0(t)] \tag{5}$$

where $\varphi_i(t) = \frac{p_{si}(t) - p_0(t)}{\rho_i(t)} = [\cos\phi_i(t) \sin\phi_i(t)]^T$ is the unit vector from the target pointing to the onboard sensor, and $\phi_i(t)$ is the bearing angle of vector $\varphi_i(t)$ as shown in Fig. 1. The unit vector $\bar{\varphi}_i(t) = [\cos(\phi_i(t) \pm \frac{\pi}{2}) \sin(\phi_i(t) \pm \frac{\pi}{2})]^T$ is orthogonal to $\varphi_i(t)$, where $\pm \frac{\pi}{2}$ denotes the opposite directions.

Assumption 1: The target's velocity and acceleration are bounded, i.e., $||v_0|| \leq \varrho_1$ and $||\dot{v}_0|| \leq \varrho_2$ where ϱ_1 and ϱ_2 are positive constants.

A. Limited Sensing and Collision Avoidance With Target

A geometrical radius r_i centered at the position of the sensor covering the robot i is labeled as a safety region. The other safety radius of the target is labeled as r_0 . Collision avoidance and limited sensing require that

$$\underline{\rho}_i < \rho_i(t) < \bar{\rho}_i \tag{6}$$

where $\underline{\rho}_i = r_i + r_0$ and $\bar{\rho}_i$ denote the safety distance and the maximum sensing range, respectively. Define the relative distance error as

$$e_{\rho i}(t) = \rho_i(t) - r_{des,i} \tag{7}$$

where $r_{des,i}$ is the desired radius centered at the target. Substituting (7) into (6) yields

$$-\underline{e}_{\rho i} < e_{\rho i}(t) < \bar{e}_{\rho i} \tag{8}$$

where $\underline{e}_{\rho i} = r_{des,i} - \underline{\rho}_i$ and $\bar{e}_{\rho i} = \bar{\rho}_i - r_{des,i}$ with $0 < \underline{\rho}_i < r_{des,i} < \bar{\rho}_i$.

Assumption 2: At the initial time t=0, the robot $i, i \in \mathcal{N}$ does not violate the constraint requirement on the relative distance, that is, $\underline{\rho}_i < \rho_i(0) < \overline{\rho}_i$ holds.

B. Collision Avoidance With Neighbouring Robots

For convenience of presentation, define the index set $\bar{\mathcal{N}}=\mathcal{N}\setminus n$. The encircling speed is assigned to any robot in the group, and this robot is labeled as robot n. Then, its previous neighbor is labeled as robot n-1 in the clockwise or counterclockwise radial order around the target p_0 according to the encircling motion direction until all robots are well defined. In terms of this definition, the robot $i,\ i\in\bar{\mathcal{N}}$, has its nextneighbouring robot i+1 labeled as i_+ . According to the arc length formula, the collision avoidance between neighbouring robots is established resulted from the minimal radius $\underline{\rho}_i$ and the corresponding minimal included angle. As shown in Fig. 1, the included angle $\alpha_{i,i+}(t)$ between robot $i,\ i\in\bar{\mathcal{N}}$, and its next-neighbouring robot i_+ can be calculated as

$$\alpha_{i,i_{+}}(t) = \cos^{-1}\left(\frac{p_{0i}^{T}(t)p_{0i_{+}}(t)}{||p_{0i}(t)||||p_{0i_{+}}(t)||}\right)$$

where $p_{0i}(t) = p_{si}(t) - p_0(t)$, $p_{0i_+}(t) = p_{si_+}(t) - p_0(t)$, and \cos^{-1} is the *inverse cosine* function. The robot $i, i \in \bar{\mathcal{N}}$, is

assumed to have access to the relative position of the target and its next-neighbour robot i_+ via an onboard sensor, e.g., a laser radar, such that their included angle is computable. For inter-robot collision avoidance, the constraint of minimal included angle $\underline{\alpha}_{i,i_+}$ is imposed on the included angle $\alpha_{i,i_+}(t)$ between the robot $i, i \in \overline{\mathcal{N}}$, and its neighbour i_+ , that is,

$$\underline{\alpha}_{i,i_{+}} < \alpha_{i,i_{+}}(t). \tag{9}$$

According to the neighbouring robot definition, the first robot (robot 1) is the next-neighbour of the last robot (robot n). However, constraint (9) is not imposed on their included angle, since robot n is designed to circle the moving target independent to the others. Define their included angle $\alpha_{n,1}$ and in view of the definition of neighbouring robots, we obtain

$$\alpha_{n,1}(t) = 2\pi - \sum_{i \in \bar{\mathcal{N}}} \alpha_{i,i_+}(t) \tag{10}$$

which implies that the included angle $\alpha_{n,1}(t)$ between the first and the last robots depends on the rest of included angles $\alpha_{i,i_+}(t)$. Moreover, the lower bound of $\alpha_{n,1}(t)$ relies on the upper bounds of $\alpha_{i,i_+}(t)$, that is, $\underline{\alpha}_{n,1} \leq 2\pi - \sum_{i \in \bar{\mathcal{N}}} \bar{\alpha}_{i,i_+}$, which prevents collision between the first and the last robots. Thus, we define the following constraint on the included angle

$$\alpha_{i,i_{+}}(t) < \bar{\alpha}_{i,i_{+}}.$$

Therefore, the following inequality

$$\underline{\alpha}_{i,i_{+}} < \alpha_{i,i_{+}}(t) < \bar{\alpha}_{i,i_{+}} \tag{11}$$

is required to prevent collisions between each robot and its next neighbour, where $\underline{\alpha}_{i,i_+}$ and $\bar{\alpha}_{i,i_+}$ are respectively the minimal and maximal included angles. Define the included angle error as

$$e_{\alpha i}(t) = \alpha_{i,i_+}(t) - \alpha_{des,i,i_+} \tag{12}$$

where α_{des,i,i_+} is the desired included angle. Substituting (12) into (11) produces

$$-\underline{e}_{\alpha i} < e_{\alpha i}(t) < \bar{e}_{\alpha i} \tag{13}$$

where $\underline{e}_{\alpha i} = \alpha_{des,i,i_+} - \underline{\alpha}_{i,i_+}$ and $\bar{e}_{\alpha i} = \bar{\alpha}_{i,i_+} - \alpha_{des,i,i_+}$ with $0 < \underline{\alpha}_{i,i_+} < \alpha_{des,i,i_+} < \bar{\alpha}_{i,i_+}$.

Remark 1: According to the definition of neighbouring robots, the desired included angles α_{des,i,i_+} correspond to the encirclement of the target, and we know that $\alpha_{des,n,1}=2\pi-\sum_{i\in\bar{\mathcal{N}}}\alpha_{des,i,i_+}$, which implies that the desired included angle $\alpha_{des,n,1}$ between the first and the last robots is not specified and relies on α_{des,i,i_+} , $i\in\bar{\mathcal{N}}$. Thus, in view of (10), the included angle error $e_{\alpha n}(t)=\alpha_{n,1}(t)-\alpha_{des,n,1}=-\sum_{i\in\bar{\mathcal{N}}}e_{\alpha i}(t)$, which indicates that the included angle error $e_{\alpha n}(t)$ depends on the sum of included angle errors between each robot $i, i\in\bar{\mathcal{N}}$, and its next-neighbouring robot i_+ . Hence, the small error $e_{\alpha n}(t)$ requires that all errors $e_{\alpha i}(t)$, $i\in\bar{\mathcal{N}}$, converge to a small neighborhood of zero.

Assumption 3: At the initial time t=0, the robot $i, i \in \bar{\mathcal{N}}$, does not violate the constraints imposed on the included angles, i.e., $\underline{\alpha}_{i,i_{+}} < \alpha_{i,i_{+}}(0) < \bar{\alpha}_{i,i_{+}}$.

It is clear from Assumption 3 and the neighbouring robot definition that the inter-robot collision along radial direction will not happen for $t \geq 0$ if the designed control laws guarantee the included angle constraints (11).

C. Formation Precision

The formation precision requires that the robots maintain the desired spacing formation to surround a target even when their encircling motions are blocked by obstacles. Accordingly, the included angle error (12) is further restricted by

$$-\Omega_{\alpha i}(t) < e_{\alpha i}(t) < \bar{\Omega}_{\alpha i}(t), \ i \in \bar{\mathcal{N}}$$
 (14)

where $\underline{\Omega}_{\alpha i}(t) > 0$ and $\bar{\Omega}_{\alpha i}(t) > 0$ are the designed decreasing \mathcal{C}^1 functions such that the included angle error $e_{\alpha i}(t)$ is driven to a small neighbourhood of zero as time evolves. Moreover, the constraint requirement (14) should satisfy the angle error constraint (13), that is, the following inequality

$$-\underline{e}_{\alpha i} \le -\underline{\Omega}_{\alpha i}(t) < e_{\alpha i}(t) < \bar{\Omega}_{\alpha i}(t) \le \bar{e}_{\alpha i}, \ i \in \bar{\mathcal{N}}$$
 (15)

is satisfied. It is clear that if the constraint requirement (14) is guaranteed by the designed controller, the inequality (13) holds, and thus the constraint imposed on the included angle (11) is never violated. A brief summary of different types of constraints considered in this work can be seen in Table I.

TABLE I

Constraint Types	Constrained Objects	Purposes	Eq. No.
Safety Constraints	Relative Distances	To avoid collisions with the target and neighbouring	(6)
	Included Angles	robots, and to guarantee limited sensing requirements.	(11)
Precision Constraints	Included Angle Errors	To ensure convergence to a small neighbourhood of the desired spacing formation.	(14)

Remark 2: When obstacles block the enclosing motion, the robots are expected to shrink their enclosing radii to surround the target and avoid obstacles simultaneously. This implies that the formation error (7) in the radial direction is expected to deviate from the origin due to the higher priority of obstacle avoidance, but the safety constraint (8) cannot be violated. Thus, the precise formation only requires that the included angle should not deviate much from its desired value, which indicates the desired spacing is maintained during the motion.

Remark 3: As discussed in Remark 1, small included angle errors $e_{\alpha i}$, $i \in \bar{\mathcal{N}}$ are preferred, such that $e_{\alpha n}(t)$ converges to a small neighbourhood of the origin. Thus, the precision constraint (14) is further designed to ensure that included angle errors should not deviate much from zero. As a result, the robots are driven to surround a moving target with a precise spacing formation in obstacle environments, despite the lack of accurate knowledge of target's velocity.

Enclosing Control Objective: The enclosing control objective is to design cooperative control laws for robot $i, i \in \mathcal{N}$, such that:

- (i) the robot *i* avoids collisions with the target, neighbouring robots, and obstacles, while guaranteeing the limited sensing requirements during the encircling motion; and
- (ii) the included angle error $e_{\alpha i}(t)$ will converge to a small neighbourhood of zero with or without obstacles.

III. MOVING-TARGET ENCLOSING CONTROL DESIGN

This section presents a constructive design technique of moving-target enclosing control for system (1) to achieve the control objective mentioned above. Although there are more than one moving obstacles in the environment, the proposed control algorithm only considers to avoid the nearest one (shown in Fig. 1), whose velocity is governed by $\dot{p}_{ob}(t) = v_{ob}(t)$ with $p_{ob}(t) = [x_{ob}(t) \ y_{ob}(t)]^T \in \mathbb{R}^2$ and $v_{ob}(t) \in \mathbb{R}^2$ being the position and velocity, respectively. The relative distance between the target and the nearest obstacle is defined as

$$\rho_{0c}(t) = \sqrt{(x_0(t) - x_{ob}(t))^2 + (y_0(t) - y_{ob}(t))^2}$$
 (16)

where the positions $p_0(t) = [x_0(t) \ y_0(t)]^T$ and $p_{ob}(t) = [x_{ob}(t) \ y_{ob}(t)]^T$ can be measured by an onboard sensor, e.g., a laser radar. For encircling motion, define that the robot's orbit is a set of positions $\{p_{si}^{'}(t)|\ ||p_{si}^{'}(t)-p_0(t)||=\rho_i(t)\}$, which describes a circle centered at the target $p_0(t)$ with radius $\rho_i(t)$. Thus, the position $p_{si}^*(t) = [x_{si}^*(t) \ y_{si}^*(t)]^T$, which is the crosspoint of target-obstacle connecting line and the orbit (shown in Fig. 1), corresponds to the shortest distance $\rho_i^*(t)$ from positions $p_{si}^{'}(t)$ to the obstacle. The relative distance between the position $p_{si}^*(t)$ and the obstacle is given by

$$\rho_i^*(t) = \sqrt{(x_{si}^*(t) - x_{ob}(t))^2 + (y_{si}^*(t) - y_{ob}(t))^2}$$
 (17)

whose derivative yields

$$\dot{\rho}_i^*(t) = \varphi_i^{*T}(t)[\dot{p}_{si}^*(t) - v_{ob}(t)]$$

where $\varphi_i^*(t) = \frac{p_{si}^*(t) - p_{ob}(t)}{\rho_i^*(t)}$ is the unit vector from the obstacle pointing to $p_{si}^*(t)$, and $\dot{p}_{si}^*(t)$ is the velocity of robot's onboard sensor when it is exactly at position $p_{si}^*(t)$. In the presence of an obstacle, the robot $i, i \in \mathcal{N}$, is required to avoid the moving obstacle, that is,

$$r_{ci} < \rho_i^*(t) \tag{18}$$

where $r_{ci} = r_i + r_{ob}$ denotes the safety distance that allows the passage of the robot i with r_{ob} being the geometrical radius covering the nearest obstacle. Furthermore, the robot i does not take evasive action until the relative distance $\rho_i^*(t)$ is less than a pre-defined obstacle avoidance range R_{ci} , that is, $\rho_i^*(t) < R_{ci}$ with $r_{ci} < R_{ci} \le \bar{\rho}_i$. It is reasonable that the obstacle avoidance range R_{ci} is less than the limited sensing range $\bar{\rho}_i$.

Assumption 4: The obstacle's velocity is bounded, i.e., $||v_{ob}|| \le \varrho_3$ with constant $\varrho_3 > 0$.

Assumption 5: There is enough separation distance for the robot i to avoid collisions with the target and the obstacle simultaneously, that is, $\rho_{0c}(t) > \rho_i + r_{ci}$.

Remark 4: The shortest distance $\rho_i^*(t)$ defined in (17) is employed to construct the potential function (20) for obstacle avoidance. However, it is not necessarily to know the corresponding position $p_{si}^*(t)$ for calculation of $\rho_i^*(t)$. Alternatively, $\rho_i^*(t)$ can be obtained by the following geometrical relationship

$$\rho_i^*(t) = \rho_{0c}(t) - \rho_i(t) \tag{19}$$

where $\rho_{0c}(t)$ and $\rho_i(t)$ are defined in (16) and (4), respectively. Furthermore, in view of (19), Assumption 5 implies that $\rho_{0c}(t) = \rho_i^*(t) + \rho_i(t) > \underline{\rho}_i + r_{ci}$. Consequently, we obtain that

 $ho_i^*(t) > r_{ci}$ as $ho_i(t) o \underline{
ho}_i^+$, and $ho_i(t) > \underline{
ho}_i$ as $ho_i^*(t) o r_{ci}^+$, which implies $ho_i(t) o \underline{
ho}_i^+$ and $ho_i^*(t) o r_{ci}^+$ cannot occur simultaneously. Noted that $x o a^+$ denotes x tending to a with x > a, whereas $x o a^-$ denotes x tending to x o a with x o a, where x o a is a variable and x o a is a constant or a variable.

The *potential* function with respect to the shortest distance $\rho_i^*(t)$ is designed for obstacle avoidance as follows

$$V_{ci}^{*}(t) = \frac{1}{2}\delta_{i}^{*2}(t) \tag{20}$$

with

$$\delta_{i}^{*}(t) = \begin{cases} \frac{1}{\rho_{i}^{*}(t) - r_{ci}}, & r_{ci} < \rho_{i}^{*}(t) \leq M_{ci} \\ A_{ci}\rho_{i}^{*2}(t) - B_{ci}\rho_{i}^{*}(t) + C_{ci}, & M_{ci} < \rho_{i}^{*}(t) < R_{ci} \\ 0, & \rho_{i}^{*}(t) \geq R_{ci} \end{cases}$$

where $A_{ci}=\frac{27}{4(R_{ci}-r_{ci})^3},~B_{ci}=\frac{27R_{ci}}{2(R_{ci}-r_{ci})^3},~C_{ci}=\frac{27R_{ci}^2}{4(R_{ci}-r_{ci})^3},~M_{ci}=\frac{2r_{ci}+R_{ci}}{3}$ with $r_{ci}< M_{ci}< R_{ci}$ due to $r_{ci}< R_{ci}$, and $\delta_i^*(t)$ is a \mathcal{C}^1 function with respect to the relative distance $\rho_i^*(t)$. Noted that $\delta_i^*(t)$ has the following properties: i) $\delta_i^*(t)\to +\infty$ as $\rho_i^*(t)\to r_{ci}^+$, and ii) $\delta_i^*(t)=0$ as $\rho_i^*(t)\geq R_{ci}$. If $V_{ci}^*(t)$ never goes to infinity, which implies that $\rho_i^*(t)$ never tends to r_{ci}^+ , then no collision with the obstacle is guaranteed. The derivative of $\delta_i^*(t)$ along (17) produces

$$\dot{\delta}_i^*(t) = \frac{\partial \delta_i}{\partial \rho_i^*} \varphi_i^{*T}(t) [\dot{p}_{si}^*(t) - v_{ob}(t)] \tag{21}$$

with

$$\frac{\partial \delta_i^*}{\partial \rho_i^*} = \begin{cases} \frac{-1}{(\rho_i^*(t) - r_{ci})^2}, & r_{ci} < \rho_i^*(t) \le M_{ci} \\ 2A_{ci}\rho_i^*(t) - B_{ci}, & M_{ci} < \rho_i^*(t) < R_{ci} \\ 0, & \rho_i^*(t) \ge R_{ci}. \end{cases}$$

However, during the encircling motion, the robot $i, i \in \mathcal{N}$, is not always at the position $p_{si}^*(t)$. Thus, in the presented obstacle avoidance strategy, the robot i takes *evasive* action when the position $p_{si}^*(t)$ gets close the moving obstacle, which means that although the robot i is not at the position $p_{si}^*(t)$, it still moves towards the target in the direction $-\varphi_i(t)$ to avoid the obstacle. Hence, the potential function with respect to the current position is designed as

$$V_{ci}(t) = \frac{1}{2}\delta_i^2(t), \quad \dot{\delta}_i(t) = -\frac{\partial \delta_i}{\partial \rho_i^*} \varphi_i^T(t) [\dot{p}_{si}(t) - v_{ob}(t)] \quad (22)$$

where $\delta_i = \delta_i^*$ and $\frac{\partial \delta_i}{\partial \rho_i^*} = \frac{\partial \delta_i^*}{\partial \rho_i^*}$ preserve the magnitudes of (20) and (21), respectively, and $-\varphi_i(t)$ indicates $\varphi_i^*(t)$ pointing towards the target whereas $\varphi_i(t)$ pointing away from the target.

Remark 5: Consider the relative distances $\rho_i(t)$ between all positions $p_{si}'(t)$ in the orbit and the nearest obstacle. It is clear that $V_{ci}^*(\rho_i^*) > V_{ci}(\rho_i')$, since $\rho_i^*(t)$ is the shortest distance among $\rho_i(t)$, and the potential function increases with the decrease in the distance according to (20) and (21). Thus, if the designed controller guarantees $V_{pi}^*(\rho_i^*)$ never tending to infinity, which implies $r_{ci} < \rho_i^*(t) < \rho_i(t)$, then robot i at any position of the orbit will not hit the obstacle. It is interpreted from (22) that the moving obstacle is rotated around the target to a virtual position such that the virtual obstacle, robot i, and the target are collinear, where robot i lies between the target and the virtual obstacle. The virtual obstacle moves towards the robot i along the radius direction $-\varphi_i(t)$. Hence, robot i

is controlled to simultaneously avoid the target and the virtual obstacle.

To satisfy constraints (8) and (14), the following universal *barrier* function is applied in the control design

$$V_{j}(t) = \frac{1}{2}\eta_{j}^{2}(t), \ j = \rho i, \alpha i$$
 (23)

with

$$\eta_j(t) = \frac{\bar{\Omega}_j(t)\underline{\Omega}_j(t)e_j(t)}{(\bar{\Omega}_j(t) - e_j(t))(e_j(t) + \underline{\Omega}_j(t))}, \ j = \rho i, \alpha i$$

where $\eta_j(t),\ j=\rho i,\ \alpha i,$ are the *transformed error* variables, $\bar{\Omega}_{\rho i}(t)=\bar{e}_{\rho i}$ and $\underline{\Omega}_{\rho i}(t)=\underline{e}_{\rho i}$ are constants from (8), $\underline{\Omega}_{\alpha i}(t)>0$ and $\bar{\Omega}_{\alpha i}(t)>0$ are time-varying functions from (14). $\eta_j(t)$ has the following properties: i) $\eta_j(t)\to -\infty$ when $e_j(t)\to -\underline{\Omega}_j^+(t);$ ii) $\eta_j(t)\to +\infty$ when $e_j(t)\to \bar{\Omega}_j^-(t);$ and $\eta_j(t)=0$ if and only if $e_j(t)=0$.

Remark 6: It follows from (23) that when the transformed errors $\eta_j(t)$ converge to a small neighbourhood of zero, that is, $|\eta_j| \leq \varrho_j, \ j = \rho i, \alpha i$, with constants $\varrho_j > 0$, the error variables e_j converge to the sets $\{e_j : -\underline{\Lambda}_j \leq e_j \leq \bar{\Lambda}_j, \text{ as } t \to \infty\}$ where

$$\underline{\Lambda}_j = \frac{\underline{\kappa}_j + \sqrt{\underline{\kappa}_j^2 + 4\varrho_j^2 \bar{\Omega}_j \underline{\Omega}_j}}{2\varrho_i}, \ \bar{\Lambda}_j = \frac{\bar{\kappa}_j + \sqrt{\bar{\kappa}_j^2 + 4\varrho_j^2 \bar{\Omega}_j \underline{\Omega}_j}}{2\varrho_j}$$

with $\underline{\kappa}_j = -\bar{\Omega}_j \underline{\Omega}_j - \varrho_j \bar{\Omega}_j + \varrho_j \underline{\Omega}_j$ and $\bar{\kappa}_j = -\bar{\Omega}_j \underline{\Omega}_j + \varrho_j \bar{\Omega}_j - \varrho_j \underline{\Omega}_j$. Using the L' Hopital's rule, we obtain that

$$\lim_{\varrho_j \to 0} \underline{\Lambda}_j = 0, \quad \lim_{\varrho_j \to 0} \bar{\Lambda}_j = 0$$

which implies that the smallest possible value ϱ_j is preferred such that the errors e_j converge to a small neighbourhood of zero.

The derivative of η_i produces

$$\dot{\eta}_{j} = \frac{\partial \eta_{j}}{\partial \bar{\Omega}_{i}} \dot{\bar{\Omega}}_{j} + \frac{\partial \eta_{j}}{\partial \underline{\Omega}_{i}} \dot{\underline{\Omega}}_{j} + \frac{\partial \eta_{j}}{\partial e_{j}} \dot{e}_{j}, \ j = \rho i, \alpha i$$
 (24)

where

$$\begin{split} \frac{\partial \eta_j}{\partial \bar{\Omega}_j} &= \frac{-\underline{\Omega}_j e_j^2}{(\bar{\Omega}_j - e_j)^2 (e_j + \underline{\Omega}_j)}, \ \frac{\partial \eta_j}{\partial \underline{\Omega}_j} = \frac{\bar{\Omega}_j e_j^2}{(\bar{\Omega}_j - e_j) (e_j + \underline{\Omega}_j)^2} \\ \frac{\partial \eta_j}{\partial e_j} &= \frac{\bar{\Omega}_j \underline{\Omega}_j (\bar{\Omega}_j \underline{\Omega}_j + e_j^2)}{(\bar{\Omega}_j - e_j)^2 (e_j + \underline{\Omega}_j)^2}. \end{split}$$

Since the target's velocity v_0 is not available for feedback, the robot i estimates the target's velocity \hat{v}_{0i} with estimation error $\tilde{v}_{0i} = \hat{v}_{0i} - v_0$. The velocity observers are designed as

$$\dot{\hat{v}}_{0i} = \Gamma_{0i} \left(-K_{0i} \hat{v}_{0i} - \varphi_i \left(\eta_{\rho i} \frac{\partial \eta_{\rho i}}{\partial e_{\rho i}} - \delta_i \frac{\partial \delta_i}{\partial \rho_i^*} \right) \right), \ i \in \mathcal{N}$$
 (25)

with $\Gamma_{0i} = \operatorname{diag}(\sigma_{0ij}) \in \mathbb{R}^{2 \times 2}$ and $K_{0i} = \operatorname{diag}(k_{0ij}) \in \mathbb{R}^{2 \times 2}$, $j = \{1, 2\}$, where $\sigma_{0ij} > 0$, $k_{0ij} > 0$ are design parameters. The control laws for the robot $i, i \in \mathcal{N}$, are designed as

$$u_i = H_i^{-1}(\varphi_i u_{1i} + \bar{\varphi}_i u_{2i} + \hat{v}_{0i}), \ i \in \bar{\mathcal{N}}$$
 (26)

$$u_i = H_i^{-1}(\varphi_i u_{1i} + \bar{\varphi}_i \bar{\omega} \rho_i + \hat{v}_{0i}), i = n$$
 (27)

with

$$\begin{split} u_{1i} &= -k_{1i} \bigg(\frac{\partial \eta_{\rho i}}{\partial e_{\rho i}} \eta_{\rho i} - \delta_{i} \frac{\partial \delta_{i}}{\partial \rho_{i}^{*}} \bigg) \\ u_{2i} &= -k_{2i} \bar{\Omega}_{\alpha i} \underline{\Omega}_{\alpha i} \eta_{\alpha i} \rho_{i} - \frac{\partial e_{\alpha i}}{\partial \bar{\Omega}_{\alpha i}} \dot{\bar{\Omega}}_{\alpha i} \rho_{i} - \frac{\partial e_{\alpha i}}{\partial \underline{\Omega}_{\alpha i}} \dot{\underline{\Omega}}_{\alpha i} \rho_{i} \\ &- \frac{\eta_{\alpha i}}{\rho_{i}} \frac{\partial \eta_{\alpha i}}{\partial e_{\alpha i}} - \eta_{\alpha i} \frac{\partial \eta_{\alpha i}}{\partial e_{\alpha i}} \rho_{i} \end{split}$$

where $k_{1i}>0$, $k_{2i}>0$ are control gains, φ_i and $\bar{\varphi}_i$ are orthogonal unit vectors defined in (5), H_i^{-1} is the inverse matrix defined in (3), and $\bar{\omega}>0$ is a design parameter.

Remark 7: The controllers (26) and (27) indicate that the robot n is constrained by both the moving target and the obstacle via terms about $\eta_{\rho n}$ and δ_n with no constraints from other robots, while robot $i, i \in \overline{\mathcal{N}}$, is further constrained by its neighbour i_+ (terms about $\eta_{\alpha i}$ in u_{2i}). Inside the obstacle avoidance range, the robots adjust their encircling radii along φ_i to meet both constraint requirements from $\eta_{\rho i}$ and δ_i .

Consider the bearing angle $\phi_i(t)$ defined in (5), control laws (26) and (27), the dynamics of ϕ_i can be derived as

$$\dot{\phi}_i = \bar{\varphi}_i^T \frac{\dot{p}_{si} - v_0}{\rho_i} = \frac{\bar{\varphi}_i^T \tilde{v}_{0i}}{\rho_i} + \Theta_i, \ i \in \mathcal{N}$$
 (28)

where $\Theta_i = \frac{u_{2i}}{\rho_i}$, $i \in \bar{\mathcal{N}}$, and $\Theta_i = \bar{\omega}$, i = n. The dynamics of included angle α_{i,i_+} is given by

$$\dot{\alpha}_{i,i_{+}} = \dot{\phi}_{i} - \dot{\phi}_{i_{+}} = \bar{\varphi}_{i}^{T} \frac{\dot{p}_{si} - v_{0}}{\rho_{i}} - \dot{\phi}_{i_{+}}, \ i \in \bar{\mathcal{N}}$$
 (29)

where ϕ_i and ϕ_{i_+} are defined in (5), and $\dot{\phi}_i$ is given in (28). Remark 8: In terms of (2) and (27), when $\delta_n=0$ and $e_{\rho n} \to 0$, we have $\dot{p}_{sn} \to \bar{\varphi}_n \bar{\omega} r_{des,n} + \hat{v}_{0n}$. The first part means that the robot n revolves around the moving target at speed $\bar{\varphi}_n \bar{\omega} r_{des,n}$ with direction $\bar{\varphi}_n$ and magnitude $\bar{\omega} r_{des,n}$. The second part means that the robot n tracks the moving target with estimation velocity \hat{v}_{0n} . If the estimation error $\tilde{v}_{0i} \to 0$, then we have $\dot{p}_{sn} \to \bar{\varphi}_n \bar{\omega} r_{des,n} + v_0$, which further implies that $\phi_n \to \bar{\omega}$ by (28). By contrast, the controller (26) for robot $i, i \in \bar{\mathcal{N}}$, lacks the encircling speed term $\bar{\varphi}_i \bar{\omega} \rho_i$ for revolving around the moving target. In terms of (2) and (26), when $\delta_i = 0$ and $e_j(t) \rightarrow 0$, $j = \rho i$, αi , we know that $\dot{p}_{si} \rightarrow \hat{v}_{0i}$. This indicates that the robot i only tracks the moving target with estimation velocity \hat{v}_{0i} , without encircling motion. Additionally, if the estimation error $\tilde{v}_{0i} \rightarrow 0$, then $\dot{p}_{si} \rightarrow v_0$, which further implies $\phi_i \rightarrow 0$ according to (28).

Remark 9: The encircling speed $\bar{\varphi}_i \bar{\omega} \rho_i$ can be treated as an external disturbance with the direction $\bar{\varphi}_i$ and the magnitude $\bar{\omega} \rho_i$ that forces the whole formation to revolve around a moving target. Furthermore, it follows from (12) and (29) that the convergence of included angle error $e_{\alpha i}(t)$ depends on both bearing angles dynamics $\dot{\phi}_i$ and $\dot{\phi}_{i_+}$. However, the robot $i, i \in \bar{\mathcal{N}}$, only accesses to the relative position without the knowledge of $\dot{\phi}_{i_+}$ from its neighbour, while tracking the desired included angle α_{des,i,i_+} . With a higher magnitude of encircling speed, the included angle may not converge to its desired value, which implies enclosing formation distortion. To handle such a problem, the precision constraint is introduced to ensure the convergence to the desired spacing formation. Therefore, when any robot is assigned an encircling speed,

the rest of robots are driven by their next-neighbouring robots to surround a moving target with small spacing errors.

The robot n is constrained by both the moving target and the obstacle without any constraint from other robots, while robot $i, i \in \bar{\mathcal{N}}$, is further constrained by its neighbour i_+ as discussed in Remark 7. Hence, Theorem 1 and Theorem 2, respectively, provide the analysis without and with the consideration of inter-robot constraints.

Theorem 1: Under Assumptions 1-2 and 4-5, consider robot kinematics (1) and system (2) with the velocity observer (25) and the control law (27) for robot n, then we have the following results.

- (i) The robot n avoids collisions with the target and obstacles, while guaranteeing the limited sensing requirements during the encircling motion.
- (ii) The control input vector $u_n(t)$ in (27) and dynamics of $\phi_n(t)$ in (28) are bounded.
- (iii) When the robot n is outside the obstacle avoidance range, i.e., $\rho_n^*(t) \geq R_{cn}$, the relative distance error $e_{\rho n}(t)$ and the estimation error $\tilde{v}_{0n}(t)$ will converge to small neighborhoods of the origin.

Proof: See Appendix A.

Theorem 2: Under Assumptions 1–5, consider robot kinematics (1) and system (2) with the velocity observer (25) and the control law (26) for robot $i, i \in \overline{\mathcal{N}}$, then we have the following results.

- (i) The robot *i* avoids collisions with the target, next-neighbouring robot, and obstacles, while guaranteeing the limited sensing requirements during the encircling motion.
- (ii) The control input vector $u_i(t)$ in (26) and dynamics of $\phi_i(t)$ in (28) are bounded.
- (iii) When the robot i is outside the obstacle avoidance range, i.e., $\rho_i^*(t) \geq R_{ci}$, the relative distance error $e_{\rho i}(t)$ and the estimation error $\tilde{v}_{0i}(t)$ will converge to small neighborhoods of the origin.
- (iv) The included angle error $e_{\alpha i}(t)$ will converge to a small neighbourhood of zero with or without obstacles.

Proof: See Appendix B.

Remark 10: In view of (46) and (47), \dot{V}_i in (47) requires the boundedness of $\dot{\phi}_{i_+}$ from the neighbour i_+ . Due to the boundedness of $\dot{\phi}_n$, \dot{V}_{n-1} in (46) can lead to (47), which implies $\dot{\phi}_{n-1}$ is bounded (Theorem 2(ii)). Hence, it is concluded that for robot $i \in \mathcal{N}$, \dot{V}_i in (47) can be obtained from (46) and $\dot{\phi}_i$ is bounded, and thus the proof is omitted.

Remark 11: When the obstacle is static, its velocity v_{ob} vanishes in the derivative of potential function (22). Accordingly, in Theorem 1(i) and Theorem 2(i), v_m in (31) and (42) is replaced by v_0 , with $||v_0|| \leq \varrho_1$ (Assumption 1). The analysis of static obstacle avoidance is similar to the proof of Theorems 1-2 under the same control strategy (25)–(27), and then is omitted here.

IV. SIMULATION STUDIES

Simulation studies of a group of five nonholonomic mobile robots are conducted using the control laws (25) and (27) for the robot 5, and (25) and (26) for the robot i, $i \in \{1, ..., 4\}$.

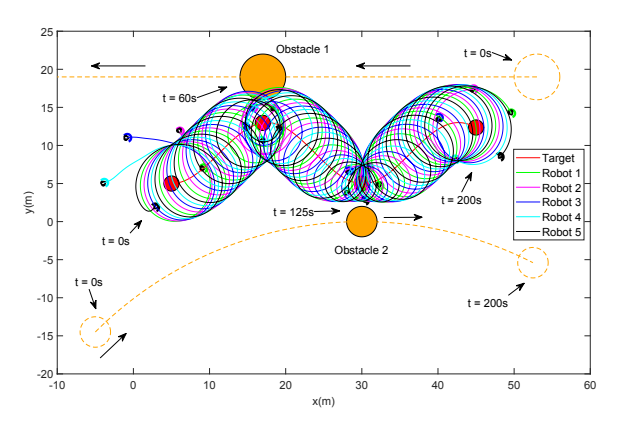


Fig. 2. The phase-plane trajectories of robots, target, and obstacles.

Let the index set $\mathcal{N}_s = \{1, ..., 5\}$ and $\bar{\mathcal{N}}_s = \mathcal{N}_s \setminus 5$. The target moves from the initial position $p_0(0) = \begin{bmatrix} 5 \end{bmatrix}^T$. The target's velocity is given by $v_0 = [0.2 \ 0.2 \sin(0.05t)]^T$ m/s which is unknown to all robots. In an obstacle environment, there are two moving obstacles whose geometrical radii are $r_{ob1} = 3$ m and $r_{ob2} = 2m$, respectively. They move from the positions $p_{ob1} = [53 \ 19]^T$ and $p_{ob2} = [-5 \ 35(1 - \sqrt{2})]^T$, respectively, with the velocities $v_{ob1} = \begin{bmatrix} 0 & -0.6 \end{bmatrix}^T$ m/s and $v_{ob2} = \begin{bmatrix} 0 & -0.6 \end{bmatrix}^T$ $[7\sqrt{2}\pi\cos(2\pi/1000t - \pi/4)/100 - 7\sqrt{2}\pi\sin(2\pi/1000t - \pi/4)]$ $(\pi/4)/100$ ^T m/s. We set the maximal sensing range $\bar{\rho}_i = 30$ m, and the safety radii of the target and robot i being $r_0 = 1$ m and $r_i = 0.5$ m, $i \in \mathcal{N}_s$, respectively. Thus, the safety distance is $\rho_{i} = 1.5$ m. Moreover, the included angle is restricted by $\underline{\alpha}_{i,i_+}=\pi/6$ rad and $\bar{\alpha}_{i,i_+}=11\pi/24$ rad, $i\in\bar{\mathcal{N}}_s$, such that $\underline{\alpha}_{5,1}=\pi/6$ rad. We chose the obstacle avoidance range $R_{ci}=15\text{m}$, the desired radius $r_{des,i}=5\text{m}$, $i\in\mathcal{N}_s$, and the desired included angle $\alpha_{des,i,i_+}=2\pi/5\mathrm{rad},\ i\in\bar{\mathcal{N}}_s.$ In view of (14), the included angle error is further restricted by the following user-defined precision constraint functions

$$\underline{\Omega}_{\alpha i}(t) = (\underline{e}_{\alpha i} - 0.005) \exp(-0.6t) + 0.005$$

$$\bar{\Omega}_{\alpha i}(t) = (\bar{e}_{\alpha i} - 0.005) \exp(-0.6t) + 0.005$$

where $\underline{e}_{\alpha i} = \alpha_{des,i,i_+} - \underline{\alpha}_{i,i_+} = 7\pi/30$ and $\bar{e}_{\alpha i} = \bar{\alpha}_{i,i_+} - \alpha_{des,i,i_+} = 7\pi/120$ according to (13). The onboard sensor is shifted by d=0.2m, and the design parameters are selected as $k_{1i}=5,\,k_{2i}=1,\,\bar{\omega}=0.5,\,\Gamma_{0i}=\mathrm{diag}(60,60),$ and $K_{0i}=\mathrm{diag}(80,80).$ The initial states of the robots are $[x_1\ y_1\ \theta_1]^T=[9\ 7\ 0]^T,\,[x_2\ y_2\ \theta_2]^T=[6\ 12\ -\pi/3]^T,\,[x_3\ y_3\ \theta_3]^T=[-1\ 11\ 0]^T,\,[x_4\ y_4\ \theta_4]^T=[-4\ 5\ \pi/6]^T,\,[x_5\ y_5\ \theta_5]^T=[3\ 2\ -3\pi/4]^T,$ and $\hat{v}_{0i}=\hat{v}_{02}=\hat{v}_{03}=\hat{v}_{04}=\hat{v}_{05}=0.$

The simulation results are presented in Figs. 2–4. The trajectories of the target, robots, and obstacles are shown in Fig. 2, where the robot group avoids moving obstacles and encloses the target towards the desired shape. Fig. 3(a) shows that when the robots move towards the target to avoid obstacles, the relative distance errors deviate from the origin but their corresponding error bounds $-\underline{e}_{\rho i}$ and $\bar{e}_{\rho i}$ are never violated, which implies that the collision avoidance with the target and the limited sensing requirements are guaranteed. Besides, as shown in Fig. 3(b), the included angle error between each robot $i, i \in \bar{\mathcal{N}}_s$ and its next neighbour i_+ converges to a small neighborhood of the origin even though

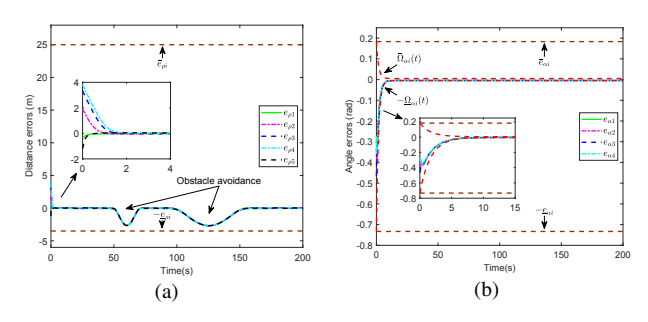


Fig. 3. The evolutions of formation errors. (a) The distance errors between each robot and moving target. (b) The included angle errors between neighbouring robots.

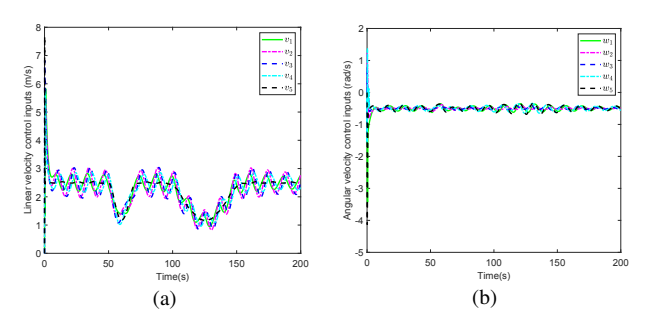


Fig. 4. The control inputs. (a) The linear velocity control inputs. (b) The angular velocity control inputs.

the robots take evasive action. This further guarantees the convergence of included angle error between the robot 1 and the robot 5 as discussed in Remark 1. It is also seen from Fig. 3(b) that all included angle errors never exceed their error bounds, which ensures the precise spacing pattern with and without the presence of obstacles. The control inputs are shown in Fig. 4.

V. CONCLUSION

This paper solves the moving-target enclosing problem for nonholonomic multirobot systems in obstacle environments with the concern of safety navigation and formation precision. A novel cooperative constrained control framework guarantees that the mobile robots can track and enclose a moving target without violating constraints from limited sensing requirements and collision avoidance with the target, neighbouring robots, and moving obstacles. The robot group can converge to a small neighborhood of the desired enclosing formation without the need of target's velocity.

VI. APPENDIX

A. Proof of Theorem 1

 ${\it Proof:}$ (i) The Lyapunov function candidate for the robot n is designed as

$$V_n = \frac{1}{2}\eta_{\rho n}^2 + \frac{1}{2}\tilde{v}_{0n}^T \Gamma_{0n}^{-1}\tilde{v}_{0n} + V_{cn}$$
 (30)

whose derivative along (2), (5), (7), (22), (24), the velocity observer (25), and the control law (27) produces

$$\dot{V}_{n} = -k_{1n} \left(\frac{\partial \eta_{\rho n}}{\partial e_{\rho n}} \eta_{\rho n} - \delta_{n} \frac{\partial \delta_{n}}{\partial \rho_{n}^{*}} \right)^{2} - \tilde{v}_{0n}^{T} K_{0n} \tilde{v}_{0n}$$

$$- \tilde{v}_{0n}^{T} K_{0n} v_{0} - \delta_{n} \frac{\partial \delta_{n}}{\partial \rho_{n}^{*}} \varphi_{n}^{T} v_{m} - \tilde{v}_{0n}^{T} \Gamma_{0n}^{-1} \dot{v}_{0}$$
(31)

where $v_m = v_0 - v_{ob}$. Under Assumptions 1 and 4, v_m is bounded, i.e., $||v_m|| \le \varrho_m$. By the completion of squares and Assumption 1, we have

$$-\tilde{v}_{0i}^T K_{0i} v_0 \le \frac{\epsilon_1^2}{2} \tilde{v}_{0i}^T K_{0i} \tilde{v}_{0i} + \frac{\lambda_{\max}(K_{0i})}{2\epsilon_1^2} \varrho_1^2$$
 (32)

$$-\tilde{v}_{0i}^{T}\Gamma_{0i}^{-1}\dot{v}_{0} \le \frac{\epsilon_{2}^{2}}{2}\tilde{v}_{0i}^{T}\Gamma_{0i}^{-1}\tilde{v}_{0i} + \frac{\lambda_{\max}(\Gamma_{0i}^{-1})}{2\epsilon_{2}^{2}}\varrho_{2}^{2}$$
 (33)

with constants $\epsilon_1 > 0$ and $\epsilon_2 > 0$. Hence (31) leads to

$$\dot{V}_{n} \leq -k_{1n} \left(\frac{\partial \eta_{\rho n}}{\partial e_{\rho n}} \eta_{\rho n} - \delta_{n} \frac{\partial \delta_{n}}{\partial \rho_{n}^{*}} \right)^{2} - \tilde{v}_{0n}^{T} G_{n} \tilde{v}_{0n} \\
- \delta_{n} \frac{\partial \delta_{n}}{\partial \rho_{n}^{*}} \varphi_{n}^{T} v_{m} + C_{n}$$
(34)

where $G_n=K_{0n}-\frac{\epsilon_1^2}{2}K_{0n}-\frac{\epsilon_2^2}{2}\Gamma_{0n}^{-1}>0$ with the proper selection of K_{0n} , Γ_{0n} , ϵ_1 , and ϵ_2 , and $C_n=\frac{\lambda_{\max}(K_{0n})}{2\epsilon_1^2}\varrho_1^2+\frac{\lambda_{\max}(\Gamma_{0n}^{-1})}{2\epsilon_2^2}\varrho_2^2$ being a positive constant. Since the potential function (22) embedded in (25) and (27) is active only inside the obstacle avoidance range, we discuss the following two cases.

Case I: When the robot n is outside the obstacle avoidance range, i.e., $\rho_n^*(t) \geq R_{cn}$, it follows $\delta_n(t) = 0$ and $\frac{\partial \delta_n}{\partial \rho_n^*} = 0$ according to (20)–(22). Thus, the Lyapunov function candidate (30) and inequality (34) become

$$V_n = \frac{1}{2}\eta_{\rho n}^2 + \frac{1}{2}\tilde{v}_{0n}^T \Gamma_{0n}^{-1}\tilde{v}_{0n}$$
(35)

$$\dot{V}_n \le -k_{1n} \left(\frac{\partial \eta_{\rho n}}{\partial e_{\rho n}}\right)^2 \eta_{\rho n}^2 - \tilde{v}_{0n}^T G_n \tilde{v}_{0n} + C_n. \tag{36}$$

It follows from (23) and (24) that

$$\left(\frac{\partial \eta_j}{\partial e_j}\right)^2 = \frac{(\bar{\Omega}_j \underline{\Omega}_j)^2 (\bar{\Omega}_j \underline{\Omega}_j + e_j^2)^2}{(\bar{\Omega}_j - e_j)^4 (e_j + \underline{\Omega}_j)^4} > \frac{1}{(\bar{\Omega}_j \underline{\Omega}_j)^2} \eta_j^4 \qquad (37)$$

where $j = \rho i, \alpha i$. As a result, (36) leads to

$$\dot{V}_n \le -k_{1n} \frac{1}{(\bar{\Omega}_{\rho n} \underline{\Omega}_{\rho n})^2} \eta_{\rho n}^6 - \tilde{v}_{0n}^T G_n \tilde{v}_{0n} + C_n. \tag{38}$$

Noted that $\bar{\Omega}_{\rho i}=\bar{e}_{\rho i}$ and $\underline{\Omega}_{\rho i}=\underline{e}_{\rho i}$ are constant. It can be concluded that $\dot{V}_n<0$ as long as either

$$\sqrt[6]{\frac{(\bar{\Omega}_{\rho n}\underline{\Omega}_{\rho n})^2C_n}{k_{1n}}} < |\eta_{\rho n}|, \text{ or } \sqrt{\frac{C_n}{\lambda_{\min}(G_n)}} < ||\tilde{v}_{0n}||.$$

Hence, V_n is nonincreasing as $\sqrt[6]{\frac{(\bar{\Omega}_{\rho n}\underline{\Omega}_{\rho n})^2C_n}{k_{1n}}} < |\eta_{\rho n}|$. It is clear from (23) and (35) that $\eta_{\rho n}$ never tends to infinity, which implies that the constraint (8) is never violated. As a result, the limited sensing requirements and collision avoidance with the target are guaranteed when $\rho_n^*(t) \geq R_{cn}$. Moreover, the error $\eta_{\rho n}$ can be reduced by increasing the gain k_{1n} .

Case II: When the robot n is inside the obstacle avoidance range, i.e., $r_{cn} < \rho_n^*(t) < R_{cn}$, it follows $\delta_n(t) > 0$ and $\frac{\partial \delta_n}{\partial \rho_n^*} < 0$. It follows from (34) that \dot{V}_n is negative outside a compact set if either $\delta_n \frac{\partial \delta_n}{\partial \sigma_n^*}$ or $\frac{\partial \eta_{\rho n}}{\partial \sigma_n^*} \eta_{\rho n}$ is bounded.

compact set if either $\delta_n \frac{\partial \delta_n}{\partial \rho_n^*}$ or $\frac{\partial \eta_{\rho n}}{\partial e_{\rho n}} \eta_{\rho n}$ is bounded. Firstly, we suppose $\delta_n \frac{\partial \delta_n}{\partial \rho_n^*}$ is bounded, i.e., $|\delta_n \frac{\partial \delta_n}{\partial \rho_n^*}| \leq c_{1n}$ with constant $c_{1n} > 0$. Consider the following inequality

$$-\delta_n \frac{\partial \delta_n}{\partial \rho_n^*} \varphi_n^T v_m \le \frac{1}{2} \left(\delta_n \frac{\partial \delta_n}{\partial \rho_n^*} \right)^2 + \frac{1}{2} v_m^T v_m$$

and then (34) leads to

$$\dot{V}_n \le -k_{1n} \left(\frac{\partial \eta_{\rho n}}{\partial e_{\rho n}} \eta_{\rho n} - \delta_n \frac{\partial \delta_n}{\partial \rho_n^*} \right)^2 - \tilde{v}_{0n}^T G_n \tilde{v}_{0n} + C_{1n}$$

where $C_{1n}=C_n+\frac{1}{2}c_{1n}^2+\frac{1}{2}\varrho_m^2$. Thus, $\dot{V}_n<0$ as long as either

$$\sqrt{\frac{C_{1n}}{k_{1n}}} < \left| \frac{\partial \eta_{\rho n}}{\partial e_{\rho n}} \eta_{\rho n} - \delta_n \frac{\partial \delta_n}{\partial \rho_n^*} \right|, \text{ or } \sqrt{\frac{C_{1n}}{\lambda_{\min}(G_n)}} < ||\tilde{v}_{0n}||.$$

Under assumption of $|\delta_n \frac{\partial \delta_n}{\partial \rho_n^*}| \leq c_{1n}$, we can obtain

$$\sqrt{\frac{C_{1n}}{k_{1n}}} + c_{1n} < \left| \frac{\partial \eta_{\rho n}}{\partial e_{\rho n}} \eta_{\rho n} \right| \Rightarrow \sqrt{\frac{C_{1n}}{k_{1n}}} < \left| \frac{\partial \eta_{\rho n}}{\partial e_{\rho n}} \eta_{\rho n} - \delta_n \frac{\partial \delta_n}{\partial \rho_n^*} \right|.$$

It is concluded that \dot{V}_n is negative as long as either $\eta_{\rho n}$ or \tilde{v}_{0n} is outside a compact set $\{\eta_{\rho n}|\frac{\partial \eta_{\rho n}}{\partial e_{\rho n}}\eta_{\rho n}\notin [-\sqrt{\frac{C_{1n}}{k_{1n}}}-c_{1n},\sqrt{\frac{C_{1n}}{k_{1n}}}+c_{1n}]\}$ or $\{\tilde{v}_{0n}|\ ||\tilde{v}_{0n}||\notin [-\sqrt{\frac{C_{1n}}{\lambda_{\min}(G_n)}},\sqrt{\frac{C_{1n}}{\lambda_{\min}(G_n)}}]\}$, which implies V_n never tends to infinity when $r_{cn}<\rho_n^*(t)< R_{cn}$. Secondly, we suppose $\frac{\partial \eta_{\rho n}}{\partial e_{\rho n}}\eta_{\rho n}$ is bounded, i.e.,

Secondly, we suppose $\frac{\partial \eta_{\rho n}}{\partial e_{\rho n}}\eta_{\rho n}$ is bounded, i.e., $|\frac{\partial \eta_{\rho n}}{\partial e_{\rho n}}\eta_{\rho n}| \leq c_{2n}$ with constant $c_{2n}>0$. Consider the following inequality

$$-\delta_n \frac{\partial \delta_n}{\partial \rho_n^*} \varphi_n^T v_m \le \frac{k_{1n}}{2} \left(\delta_n \frac{\partial \delta_n}{\partial \rho_n^*} \right)^2 + \frac{1}{2k_{1n}} v_m^T v_m$$

then (34) leads to

$$\dot{V}_n \le -k_{1n} \left(\sqrt{2} \frac{\partial \eta_{\rho n}}{\partial e_{\rho n}} \eta_{\rho n} - \frac{\sqrt{2}}{2} \delta_n \frac{\partial \delta_n}{\partial \rho_n^*} \right)^2 - \tilde{v}_{0n}^T G_n \tilde{v}_{0n} + C_{2n}$$

where $C_{2n}=C_n+k_{1n}c_{2n}^2+\frac{1}{2k_{1n}}\varrho_m^2$. Thus, $\dot{V}_n<0$ as long as either

$$\sqrt{\frac{C_{2n}}{k_{1n}}} < \left| \sqrt{2} \frac{\partial \eta_{\rho n}}{\partial e_{\rho n}} \eta_{\rho n} - \frac{\sqrt{2}}{2} \delta_n \frac{\partial \delta_n}{\partial \rho_n^*} \right|, \text{ or } \sqrt{\frac{C_{2n}}{\lambda_{\min}(G_n)}} < ||\tilde{v}_{0n}||.$$

Under assumption of $\left|\frac{\partial \eta_{\rho n}}{\partial e_{\rho n}}\eta_{\rho n}\right| \leq c_{2n}$, we have

$$\sqrt{\frac{C_{2n}}{k_{1n}}} + \sqrt{2}c_{2n} < \frac{\sqrt{2}}{2} \left| \delta_n \frac{\partial \delta_n}{\partial \rho_n^*} \right|$$

which implies

$$\sqrt{\frac{C_{2n}}{k_{1n}}} < \left| \sqrt{2} \frac{\partial \eta_{\rho n}}{\partial e_{\rho n}} \eta_{\rho n} - \frac{\sqrt{2}}{2} \delta_n \frac{\partial \delta_n}{\partial \rho_n^*} \right|.$$

It is concluded that \dot{V}_n is negative as long as either δ_n or \tilde{v}_{0n} is outside a compact set $\{\delta_n|\ \delta_n\frac{\partial \delta_n}{\partial \rho_n^*}\notin [-\sqrt{\frac{2C_{2n}}{k_{1n}}}-2c_{2n},\ \sqrt{\frac{2C_{2n}}{k_{1n}}}+2c_{2n}\]\}$ or $\{\tilde{v}_{0n}|\ ||\tilde{v}_{0n}||\notin \mathbb{R}\}$

 $[-\sqrt{\frac{C_{2n}}{\lambda_{\min}(G_n)}},\ \sqrt{\frac{C_{2n}}{\lambda_{\min}(G_n)}}\]\}, \ \text{which implies}\ V_n \ \textit{never} \ \text{tends}$ to infinity when $r_{cn}<\rho_n^*(t)< R_{cn}.$ Therefore, V_n may go to infinity as both $\delta_n\frac{\partial \delta_n}{\partial \rho_n^*}$ and $\frac{\partial \eta_{\rho n}}{\partial e_{\rho n}}\eta_{\rho n}$

Therefore, V_n may go to infinity as both $\delta_n \frac{\partial \delta_n}{\partial \rho_n^*}$ and $\frac{\partial \eta_{\rho n}}{\partial e_{\rho n}} \eta_{\rho n}$ go to infinity. Next, we discuss the case that both $\delta_n \frac{\partial \delta_n}{\partial \rho_n^*}$ and $\frac{\partial \eta_{\rho n}}{\partial e_{\rho n}} \eta_{\rho n}$ tend to infinity with the same and opposite signs. Consider the following inequality

$$-\delta_n \frac{\partial \delta_n}{\partial \rho_n^*} \varphi_n^T v_m \le k_{1n} \left(\delta_n \frac{\partial \delta_n}{\partial \rho_n^*} \right)^2 + \frac{1}{4k_{1n}} v_m^T v_m$$

then (34) leads to

$$\dot{V}_{n} \leq -k_{1n} \left(\frac{\partial \eta_{\rho n}}{\partial e_{\rho n}} \eta_{\rho n} - \delta_{n} \frac{\partial \delta_{n}}{\partial \rho_{n}^{*}} \right)^{2} + k_{1n} \left(\delta_{n} \frac{\partial \delta_{n}}{\partial \rho_{n}^{*}} \right)^{2} - \tilde{v}_{0n}^{T} G_{n} \tilde{v}_{0n} + C_{3n}$$

where $C_{3n}=C_n+\frac{1}{4k_{1n}}\varrho_m^2$. Thus, $\dot{V}_n<0$ as long as either $C_{3n}< k_{1n}\left(\frac{\partial\eta_{\rho n}}{\partial e_{\rho n}}\eta_{\rho n}\right)\left(\frac{\partial\eta_{\rho n}}{\partial e_{\rho n}}\eta_{\rho n}-2\delta_n\frac{\partial\delta_n}{\partial\rho_n^*}\right)$ or $C_{3n}<\tilde{v}_{0n}^TG_n\tilde{v}_{0n}$. It is clear that when $\frac{\partial\eta_{\rho n}}{\partial e_{\rho n}}\eta_{\rho n}\to\infty$ and $\delta_n\frac{\partial\delta_n}{\partial\rho_n^*}\to\infty$ with opposite sign, we have $\delta_n\frac{\partial\delta_n}{\partial\rho_n^*}\frac{\partial\eta_{\rho n}}{\partial e_{\rho n}}\eta_{\rho n}\to-\infty$, which implies

$$k_{1n} \left(\frac{\partial \eta_{\rho n}}{\partial e_{\rho n}} \eta_{\rho n} \right) \left(\frac{\partial \eta_{\rho n}}{\partial e_{\rho n}} \eta_{\rho n} - 2\delta_n \frac{\partial \delta_n}{\partial \rho_n^*} \right) \to +\infty.$$

Consequently, before both $\frac{\partial \eta_{\rho n}}{\partial e_{\rho n}} \eta_{\rho n}$ and $\delta_n \frac{\partial \delta_n}{\partial \rho_n^*}$ simultaneously tending to infinity with opposite sign, we can find $\forall \frac{\partial \eta_{\rho n}}{\partial e_{\rho n}} \eta_{\rho n} \notin \Omega_{\eta n}$ and $\forall \delta_n \frac{\partial \delta_n}{\partial \rho_n^*} \notin \Omega_{\delta n}$ where $\Omega_{\eta n}$ and $\Omega_{\delta n}$ are compact subsets of $\mathbb R$ containing the origin such that

$$\frac{C_{3n}}{k_{1n}} < \left(\frac{\partial \eta_{\rho n}}{\partial e_{\rho n}} \eta_{\rho n}\right) \left(\frac{\partial \eta_{\rho n}}{\partial e_{\rho n}} \eta_{\rho n} - 2\delta_n \frac{\partial \delta_n}{\partial \rho_n^*}\right)$$

which implies that $\dot{V}_n < 0$ when both $\frac{\partial \eta_{\rho n}}{\partial e_{\rho n}} \eta_{\rho n}$ and $\delta_n \frac{\partial \delta_n}{\partial \rho_n^*}$ are, respectively, outside compact sets $\Omega_{\eta n}$ and $\Omega_{\delta n}$. It is concluded that $\dot{V}_n < 0$ before both $\frac{\partial \eta_{\rho n}}{\partial e_{\rho n}} \eta_{\rho n}$ and $\delta_n \frac{\partial \delta_n}{\partial \rho_n^*}$ simultaneously tend to infinity with opposite sign, or as v_{0n} is outside a compact set, that is, $\{(\eta_{\rho n}, \delta_n)| \frac{\partial \eta_{\rho n}}{\partial e_{\rho n}} \eta_{\rho n} \notin \Omega_{\eta n}, \delta_n \frac{\partial \delta_n}{\partial \rho_n^*} \notin \Omega_{\delta n} \}$ or $\{\tilde{v}_{0n}| ||\tilde{v}_{0n}|| \notin [-\sqrt{\frac{C_{3n}}{\lambda_{\min}(G_n)}}, \sqrt{\frac{C_{3n}}{\lambda_{\min}(G_n)}}]\}$, which implies V_n never tends to infinity when $r_{cn} < \rho_n^*(t) < R_{cn}$. Next, we show that both $\frac{\partial \eta_{\rho n}}{\partial e_{\rho n}} \eta_{\rho n}$ and $\delta_n \frac{\partial \delta_n}{\partial \rho_n^*}$ tending to infinity with the same sign will not happen. Noted that $\delta_n(t) >$

Next, we show that both $\frac{\partial \eta_{\rho n}}{\partial e_{\rho n}} \eta_{\rho n}$ and $\delta_n \frac{\partial \delta_n}{\partial \rho_n^*}$ tending to infinity with the *same* sign will not happen. Noted that $\delta_n(t) > 0$ and $\frac{\partial \delta_n}{\partial \rho_n^*} < 0$ when $r_{cn} < \rho_n^*(t) < R_{cn}$, and we obtain from (20) and (21) that

$$\delta_n \frac{\partial \delta_n}{\partial \rho_n^*} \to -\infty \text{ as } \rho_n^* \to r_{cn}^+.$$

Furthermore, it follows from (24) that $\frac{\partial \eta_{pn}}{\partial e_{pn}} > 0$, and in view of (7), (8), and (23), we have

$$\frac{\partial \eta_{\rho n}}{\partial e_{\rho n}} \eta_{\rho n} \to -\infty \text{ as } \rho_n \to \underline{\rho}_n^+, \ \frac{\partial \eta_{\rho n}}{\partial e_{\rho n}} \eta_{\rho n} \to +\infty \text{ as } \rho_n \to \bar{\rho}_n^-.$$

Thus, when $\rho_n^* \to r_{cn}^+$ and $\rho_n \to \underline{\rho}_n^+$ simultaneously, both $\frac{\partial \eta_{\rho n}}{\partial e_{\rho n}} \eta_{\rho n}$ and $\delta_n \frac{\partial \delta_n}{\partial \rho_n^*}$ have the same sign, tending to negative infinity. In view of Assumption 5 and Remark 4, $\rho_n^* \to r_{cn}^+$ and $\rho_n \to \underline{\rho}_n^+$ simultaneously cannot occur. As a result, V_n never goes to infinity when the robot n is inside the obstacle

avoidance range. Therefore, the limited sensing requirements, and collision avoidance with both the target and the obstacle are guaranteed when $r_{cn} < \rho_n^*(t) < R_{cn}$.

(ii) It is clear from the Theorem 1(i) that V_n in (30) never tends to infinity, which implies that its arguments $\eta_{\rho n}$, \tilde{v}_{0n} , and δ_n are bounded. The boundedness of $\eta_{\rho n}$ indicates the boundedness of $e_{\rho n}$ in view of (8) and (23), which further implies $0<\underline{\rho}_n<\bar{\rho}_n$ according to (6). The boundedness of $\eta_{\rho n}$ also implies that $\frac{\partial \eta_{\rho n}}{\partial e_{\rho n}}$ is bounded. Besides, it is clear from (20) that the boundedess of δ_n guarantees $r_{cn}<\rho_n^*$, and thus $\frac{\partial \delta_n}{\partial \rho_n^*}$ is bounded. As a result, it is easy to verify from (27) and (28) that signals u_n and $\dot{\phi}_n$ are bounded.

(iii) Completing the squares, for any variable $x \in \mathbb{R}$, we have $(x^3 - x)^2 \ge 0$ and $(x^2 - 1)^2 \ge 0$, which produces

$$-x^6 < -3x^2 + 2. (39)$$

Consider \dot{V}_n in (38) when the robot n is outside the obstacle avoidance range. Substituting (39) into (38) yields

$$\dot{V}_n \le -3k_{1n}^{\frac{1}{3}}(\bar{\Omega}_{\rho n}\underline{\Omega}_{\rho n})^{-\frac{2}{3}}\eta_{\rho n}^2 - \tilde{v}_{0n}^TG_n\tilde{v}_{0n} + \bar{C}_n$$

where $\bar{C}_n=C_n+2$. Thus, we obtain $\dot{V}_n\leq -\mu_n V_n+\bar{C}_n$ from (35), where $\mu_n=\min\{6k_{1n}^{\frac{1}{3}}(\bar{\Omega}_{\rho n}\underline{\Omega}_{\rho n})^{-\frac{2}{3}},2\frac{\lambda_{\min}(G_n)}{\lambda_{\max}(\Gamma_{0n}^{-1})}\}$, which implies that

$$V_n(t) \le \left(V_n(0) - \frac{\bar{C}_n}{\mu_n}\right) e^{-\mu_n t} + \frac{\bar{C}_n}{\mu_n}.$$

It is further from (35) that as $t \to \infty$, we obtain $\frac{1}{2}\eta_{\rho n}^2 \le \frac{\bar{C}_n}{\mu_n}$ and $\frac{1}{2}\tilde{v}_{0n}^T\Gamma_{0n}^{-1}\tilde{v}_{0n} \le \frac{\bar{C}_n}{\mu_n}$, which produces

$$|\eta_{\rho n}| \le \sqrt{\frac{2\bar{C}_n}{\mu_n}}, \ ||\tilde{v}_{0n}|| \le \sqrt{\frac{2\bar{C}_n}{\mu_n \lambda_{\min}(\Gamma_{0n}^{-1})}}.$$
 (40)

As discussed in Remark 6, to ensure the convergence set of relative distance error $\{e_{\rho n}: -\underline{\Lambda}_{\rho n} \leq e_{\rho n} \leq \bar{\Lambda}_{\rho n}, \text{ as } t \to \infty\}$ being small, it is desirable that $|\eta_{\rho n}| \leq \varrho_{\rho n}$ in (40), with $\varrho_{\rho n} = \sqrt{\frac{2\bar{C}_n}{\mu_n}}$ being small as possible. Thus, small \bar{C}_n and large μ_n are preferred by selecting large gains k_{1n} and Γ_{0n} such that the relative distance error $e_{\rho n}(t)$ and the estimation error $\tilde{v}_{0n}(t)$ will converge to small neighborhoods of the origin when $\rho_n^*(t) \geq R_{cn}$.

B. Proof of Theorem 2

Proof: (i) The Lyapunov function candidate for the robot i, $i \in \bar{\mathcal{N}}$, is chosen as

$$V_{i} = \frac{1}{2}\eta_{\rho i}^{2} + \frac{1}{2}\eta_{\alpha i}^{2} + \frac{1}{2}\tilde{v}_{0i}^{T}\Gamma_{0i}^{-1}\tilde{v}_{0i} + V_{ci}$$
 (41)

whose derivative along (2), (5), (7), (12), (22), (24), (29), the velocity observer (25), and the control law (26) produces

$$\dot{V}_{i} = -k_{1i} \left(\frac{\partial \eta_{\rho i}}{\partial e_{\rho i}} \eta_{\rho i} - \delta_{i} \frac{\partial \delta_{i}}{\partial \rho_{i}^{*}} \right)^{2} - k_{2i} \bar{\Omega}_{\alpha i} \underline{\Omega}_{\alpha i} \frac{\partial \eta_{\alpha i}}{\partial e_{\alpha i}} \eta_{\alpha i}^{2}
- \tilde{v}_{0i}^{T} K_{0i} \tilde{v}_{0i} + \eta_{\alpha i} \frac{\partial \eta_{\alpha i}}{\partial e_{\alpha i}} \frac{\bar{\varphi}_{i}^{T} \tilde{v}_{0i}}{\rho_{i}} - \left(\frac{\eta_{\alpha i}}{\rho_{i}} \frac{\partial \eta_{\alpha i}}{\partial e_{\alpha i}} \right)^{2}
- \delta_{i} \frac{\partial \delta_{i}}{\partial \rho_{i}^{*}} \varphi_{i}^{T} v_{m} - \eta_{\alpha i} \frac{\partial \eta_{\alpha i}}{\partial e_{\alpha i}} \dot{\phi}_{i_{+}} - \left(\eta_{\alpha i} \frac{\partial \eta_{\alpha i}}{\partial e_{\alpha i}} \right)^{2}
- \tilde{v}_{0i}^{T} K_{0i} v_{0} - \tilde{v}_{0i}^{T} \Gamma_{0i}^{-1} \dot{v}_{0}.$$
(42)

Completing the squares, we obtain

$$\eta_{\alpha i} \frac{\partial \eta_{\alpha i}}{\partial e_{\alpha i}} \frac{\bar{\varphi}_{i}^{T} \tilde{v}_{0i}}{\rho_{i}} \leq \frac{\epsilon_{\alpha_{1}}^{2}}{2} \left(\frac{\eta_{\alpha i}}{\rho_{i}} \frac{\partial \eta_{\alpha i}}{\partial e_{\alpha i}} \right)^{2} + \frac{1}{2\epsilon_{\alpha_{1}}^{2}} \tilde{v}_{0i}^{T} \tilde{v}_{0i}$$
(43)

$$-\eta_{\alpha i} \frac{\partial \eta_{\alpha i}}{\partial e_{\alpha i}} \dot{\phi}_{i+} \le \frac{\epsilon_{\alpha_2}^2}{2} \left(\eta_{\alpha i} \frac{\partial \eta_{\alpha i}}{\partial e_{\alpha i}} \right)^2 + \frac{1}{2\epsilon_{\alpha_2}^2} \dot{\phi}_{i+}^2. \tag{44}$$

Moreover, it follows from (23) and (24) that

$$\bar{\Omega}_{j}\underline{\Omega}_{j}\frac{\partial \eta_{j}}{\partial e_{j}} = \frac{(\bar{\Omega}_{j}\underline{\Omega}_{j})^{2}(\bar{\Omega}_{j}\underline{\Omega}_{j} + e_{j}^{2})}{(\bar{\Omega}_{j} - e_{j})^{2}(e_{j} + \underline{\Omega}_{j})^{2}} > \eta_{j}^{2}$$
(45)

where $j = \rho i, \alpha i$. Using the inequalities (32), (33), (43), (44), and (45), (42) leads to

$$\dot{V}_{i} \leq -k_{1i} \left(\frac{\partial \eta_{\rho i}}{\partial e_{\rho i}} \eta_{\rho i} - \delta_{i} \frac{\partial \delta_{i}}{\partial \rho_{i}^{*}} \right)^{2} - k_{2i} \eta_{\alpha i}^{4} - \tilde{v}_{0i}^{T} G_{i} \tilde{v}_{0i}
- \delta_{i} \frac{\partial \delta_{i}}{\partial \rho_{i}^{*}} \varphi_{i}^{T} v_{m} + \frac{1}{2\epsilon_{\alpha 2}^{2}} \dot{\varphi}_{i_{+}}^{2} + C_{i}^{*}$$
(46)

where $G_i = K_{0i} - \frac{\epsilon_1^2}{2} K_{0i} - \frac{\epsilon_2^2}{2} \Gamma_{0i}^{-1} - \frac{1}{2\epsilon_{\alpha_1}^2} I_2 > 0, \frac{\epsilon_{\alpha_1}^2}{2} < 1$, and $\frac{\epsilon_{\alpha_2}^2}{2} < 1$ with the proper selection of K_{0n} , Γ_{0n} , ϵ_1 , ϵ_2 , and ϵ_{α_1} , and $C_i^* = \frac{\lambda_{\max}(K_{0i})}{2\epsilon_1^2} \varrho_1^2 + \frac{\lambda_{\max}(\Gamma_{0i}^{-1})}{2\epsilon_2^2} \varrho_2^2$ being a positive constant. Since the boundedness of $\dot{\phi}_{i_+}$, i.e., $|\dot{\phi}_{i_+}| \leq c_{i_+}$ with constant $c_{i+} > 0$, inequality (46) gives

$$\dot{V}_{i} \leq -k_{1i} \left(\frac{\partial \eta_{\rho i}}{\partial e_{\rho i}} \eta_{\rho i} - \delta_{i} \frac{\partial \delta_{i}}{\partial \rho_{i}^{*}} \right)^{2} - k_{2i} \eta_{\alpha i}^{4} - \tilde{v}_{0i}^{T} G_{i} \tilde{v}_{0i} \\
- \delta_{i} \frac{\partial \delta_{i}}{\partial \rho_{i}^{*}} \varphi_{i}^{T} v_{m} + C_{i}$$
(47)

where $C_i = C_i^* + \frac{1}{2\epsilon_{\alpha_2}^2}c_{i_+}^2$. According to Theorem 1(ii), we know that $\dot{\phi}_n$ is bounded and \dot{V}_i for the robot n-1 can lead to (47). Since the potential function (22) embedded in (25) and (26) vanishes outside the obstacle avoidance range, we also discuss the following two cases.

Case I: When the robot i is outside the obstacle avoidance range, i.e., $\rho_i^*(t) \geq R_{ci}$, we have $\delta_i(t) = 0$ and $\frac{\partial \delta_i}{\partial \rho_i^*} = 0$. Thus, the Lyapunov function candidate (41) and inequality (47) become

$$V_{i} = \frac{1}{2}\eta_{\rho i}^{2} + \frac{1}{2}\eta_{\alpha i}^{2} + \frac{1}{2}\tilde{v}_{0i}^{T}\Gamma_{0i}^{-1}\tilde{v}_{0i}$$

$$\tag{48}$$

$$\dot{V}_i \le -k_{1i} \left(\frac{\partial \eta_{\rho i}}{\partial e_{\rho i}}\right)^2 \eta_{\rho i}^2 - k_{2i} \eta_{\alpha i}^4 - \tilde{v}_{0i}^T G_i \tilde{v}_{0i} + C_i. \tag{49}$$

Using the inequality (37), (49) leads to

$$\dot{V}_{i} \leq -k_{1i} \frac{1}{(\bar{\Omega}_{\alpha i} \Omega_{\alpha i})^{2}} \eta_{\rho i}^{6} - k_{2i} \eta_{\alpha i}^{4} - \tilde{v}_{0i}^{T} G_{i} \tilde{v}_{0i} + C_{i}. \quad (50)$$

It can be concluded that $\dot{V}_i < 0$ as long as $\sqrt[6]{\frac{(\bar{\Omega}_{\rho i} \underline{\Omega}_{\rho i})^2 C_i}{k_{1:i}}} < 0$
$$\begin{split} |\eta_{\rho i}| \ \ \text{or} \ \ \sqrt[4]{\frac{C_i}{k_{2i}}} \ < \ |\eta_{\alpha i}| \ \ \text{or} \ \sqrt{\frac{C_i}{\lambda_{\min}(G_i)}} \ < \ ||\tilde{v}_{0i}||. \ \ \text{Hence,} \ \ V_i \\ \text{is nonincreasing as} \ \ \sqrt[6]{\frac{(\bar{\Omega}_{\rho i}\underline{\Omega}_{\rho i})^2C_i}{k_{1i}}} \ < \ |\eta_{\rho i}| \ \ \text{or} \ \ \sqrt[4]{\frac{C_i}{k_{2i}}} \ < \ |\eta_{\alpha i}|. \end{split}$$
It follows from (23) and (48) that $\eta_{\rho i}$ and $\eta_{\alpha i}$ never tend to infinity, which indicates that the constraints (8) and (13) are never violated. As a result, the limited sensing requirements, and collision avoidance with both the target and the next-neighbouring robot are guaranteed when $\rho_i^*(t) \geq R_{ci}$. Moreover, by increasing the gains k_{1i} and k_{2i} , the errors $\eta_{\rho i}$ and $\eta_{\alpha i}$ can be reduced.

Case II: When the robot i is inside the obstacle avoidance range, i.e., $r_{ci} < \rho_i^*(t) < R_{ci}$, we have $\delta_i(t) > 0$ and $\frac{\partial \delta_i}{\partial \rho_i^*} < 0$. Similar to the *Case II* of Theorem 1(i), \dot{V}_i is negative outside a compact set if either $\delta_i \frac{\partial \delta_i}{\partial \rho_i^*}$ or $\frac{\partial \eta_{\rho i}}{\partial e_{\rho i}} \eta_{\rho i}$ is bounded. For $|\delta_i \frac{\partial \delta_i}{\partial \rho_i^*}| \leq c_{1i}$ with constant $c_{1i} > 0$, (47) leads to

$$\dot{V}_i \le -k_{1i} \left(\frac{\partial \eta_{\rho i}}{\partial e_{\rho i}} \eta_{\rho i} - \delta_i \frac{\partial \delta_i}{\partial \rho_i^*} \right)^2 - k_{2i} \eta_{\alpha i}^4 - \tilde{v}_{0i}^T G_i \tilde{v}_{0i} + C_{1i}$$

where $C_{1i} = C_i + \frac{1}{2}c_{1i}^2 + \frac{1}{2}\varrho_m^2$. It is concluded that \dot{V}_i is negative when $\{\eta_{\rho i} | \frac{\partial \eta_{\rho i}}{\partial e_{\rho i}} \eta_{\rho i} \notin [-\sqrt{\frac{C_{1i}}{k_{1i}}} - c_{1i}, \sqrt{\frac{C_{1i}}{k_{1i}}} + c_{2i}\}$ c_{1i}]} or $\{\eta_{\alpha i} | \eta_{\alpha i} \notin [-\sqrt[4]{\frac{C_{1i}}{k_{2i}}}, \sqrt[4]{\frac{C_{1i}}{k_{2i}}}]\}$ or $\{\tilde{v}_{0i} | ||\tilde{v}_{0i}|| \notin$
$$\begin{split} & [-\sqrt{\frac{C_{1i}}{\lambda_{\min}(G_i)}}, \ \sqrt{\frac{C_{1i}}{\lambda_{\min}(G_i)}}\]\}. \\ & \text{For } |\frac{\partial \eta_{\rho i}}{\partial e_{oi}}\eta_{\rho i}| \leq c_{2i} \text{ with constant } c_{2i} > 0, \text{ (47) leads to} \end{split}$$

$$\dot{V}_{i} \leq -k_{1i} \left(\sqrt{2} \frac{\partial \eta_{\rho i}}{\partial e_{\rho i}} \eta_{\rho i} - \frac{\sqrt{2}}{2} \delta_{i} \frac{\partial \delta_{i}}{\partial \rho_{i}^{*}} \right)^{2} - k_{2i} \eta_{\alpha i}^{4}$$
$$- \tilde{v}_{0i}^{T} G_{i} \tilde{v}_{0i} + C_{2i}$$

where $C_{2i} = C_i + k_{1i}c_{2i}^2 + \frac{1}{2k_{1i}}\varrho_m^2$. It is concluded that \dot{V}_i is negative when $\{\delta_i | \delta_i \frac{\partial \delta_i}{\partial \rho_i^*} \notin [-\sqrt{\frac{2C_{2i}}{k_{1i}}} - 2c_{2i}, \sqrt{\frac{2C_{2i}}{k_{1i}}} +$ $2c_{2i}] \} \text{ or } \{ \eta_{\alpha i} | \eta_{\alpha i} \notin [-\sqrt[4]{\frac{C_{2i}}{k_{2i}}}, \sqrt[4]{\frac{C_{2i}}{k_{2i}}}] \} \text{ or } \{ \tilde{v}_{0i} | ||\tilde{v}_{0i}|| \notin [-\sqrt{\frac{C_{2i}}{\lambda_{\min}(G_i)}}, \sqrt{\frac{C_{2i}}{\lambda_{\min}(G_i)}}] \}.$ When both $\frac{\partial \eta_{\rho i}}{\partial e_{\rho i}} \eta_{\rho i}$ and $\delta_i \frac{\partial \delta_i}{\partial \rho_i^*}$ tend to infinity, it is clear from (47) that

$$\dot{V}_{i} \leq -k_{1i} \left(\frac{\partial \eta_{\rho i}}{\partial e_{\rho i}} \eta_{\rho i} - \delta_{i} \frac{\partial \delta_{i}}{\partial \rho_{i}^{*}}\right)^{2} + k_{1i} \left(\delta_{i} \frac{\partial \delta_{i}}{\partial \rho_{i}^{*}}\right)^{2} - k_{2i} \eta_{\alpha i}^{4} - \tilde{v}_{0i}^{T} G_{i} \tilde{v}_{0i} + C_{3i}$$

where $C_{3i}=C_i+\frac{1}{4k_{1i}}\varrho_m^2$. When $\frac{\partial \eta_{\rho i}}{\partial e_{\rho i}}\eta_{\rho i}\to\infty$ and $\delta_i\frac{\partial \delta_i}{\partial \rho_i^*}\to\infty$ with *opposite* sign, we have

$$k_{1i} \left(\frac{\partial \eta_{\rho i}}{\partial e_{\rho i}} \eta_{\rho i} \right) \left(\frac{\partial \eta_{\rho i}}{\partial e_{\rho i}} \eta_{\rho i} - 2\delta_i \frac{\partial \delta_i}{\partial \rho_i^*} \right) \to +\infty.$$

Thus, we can find $\forall \frac{\partial \eta_{\rho i}}{\partial e_{\rho i}} \eta_{\rho i} \notin \Omega_{\eta i}$ and $\forall \delta_i \frac{\partial \delta_i}{\partial \rho_i^*} \notin \Omega_{\delta i}$ where $\Omega_{\eta i}$ and $\Omega_{\delta i}$ are compact subsets of \mathbb{R} containing the origin such that

$$\frac{C_{3i}}{k_{1i}} < \left(\frac{\partial \eta_{\rho i}}{\partial e_{\rho i}} \eta_{\rho i}\right) \left(\frac{\partial \eta_{\rho i}}{\partial e_{\rho i}} \eta_{\rho i} - 2\delta_i \frac{\partial \delta_i}{\partial \rho_i^*}\right).$$

It is concluded that \dot{V}_i is negative when $\{(\eta_{\rho i},\delta_i)|\ \frac{\partial \eta_{\rho i}}{\partial e_{\rho i}}\eta_{\rho i}\notin$ $\begin{array}{l} \Omega_{\eta i}, \delta_{i} \frac{\partial \delta_{i}}{\partial \rho_{i}^{*}} \notin \Omega_{\delta i} \} \text{ or } \{\eta_{\alpha i} | \eta_{\alpha i} \notin [-\sqrt[4]{\frac{C_{3i}}{k_{2i}}}, \sqrt[4]{\frac{C_{3i}}{k_{2i}}}] \} \text{ or } \\ \{\tilde{v}_{0i} | ||\tilde{v}_{0i}|| \notin [-\sqrt{\frac{C_{3i}}{\lambda_{\min}(G_{i})}}, \sqrt{\frac{C_{3i}}{\lambda_{\min}(G_{i})}}] \}, \text{ which implies } V_{i} \end{array}$

never tends to infinity when $r_{ci} < \rho_i^*(t) < R_{ci}$. Similar to Case II of Theorem 1(i), both $\frac{\partial \eta_{\rho i}}{\partial e_{\rho i}} \eta_{\rho i}$ and $\delta_i \frac{\partial \delta_i}{\partial \rho_i^*}$ tending to infinity with the same sign will not happen. As a result, V_i never goes to infinity when the robot i is inside the obstacle avoidance range. Therefore, the limited sensing requirements, and collision avoidance with the target, nextneighbouring robot, and the obstacle are guaranteed when $r_{ci} < \rho_i^*(t) < R_{ci}.$

(ii) It is clear from Theorem 2(i) that V_i in (41) never tends to infinity, which implies that its arguments $\eta_{\rho i}$, $\eta_{\alpha i}$, \tilde{v}_{0i} , and δ_i are bounded. The boundedness of $\eta_{\rho i}$ and $\eta_{\alpha i}$, respectively, indicates the boundedness of $e_{\rho i}$ and $e_{\alpha i}$ in view of (8), (15), and (23), which further implies $0<\underline{\rho}_i<\rho_i<\bar{\rho}_i$ and $\underline{\alpha}_{i,i_+}<\alpha_{i,i_+}$ according to (6) and (11). The boundedness of $\eta_{\rho i}$ and $\eta_{\alpha i}$ also implies that $\frac{\partial \eta_{\rho i}}{\partial e_{\rho i}}$, $\frac{\partial e_{\alpha i}}{\partial \Omega_{\alpha i}}$, $\frac{\partial e_{\alpha i}}{\partial \Omega_{\alpha j}}$, and $\frac{\partial \eta_{\alpha i}}{\partial e_{\alpha i}}$ are bounded. It follows from (20) that the boundedness of δ_i guarantees $r_{ci}<\rho_i^*$, and thus $\frac{\partial \delta_i}{\partial \rho_i^*}$ is bounded. Moreover, the boundedness of $\bar{\Omega}_{\alpha i}$ and $\Omega_{\alpha i}$. As a result, it is easy to verify from (26) and (28) that signals u_i and $\dot{\phi}_i$ are bounded.

(iii) Completing the squares, for any variable $x \in \mathbb{R}$, we have $(x^2 - 1)^2 \ge 0$, which produces

$$-x^4 \le -2x^2 + 1. (51)$$

We consider \dot{V}_i given in (50) when the robot i is outside the obstacle avoidance range. Substituting (39) and (51) into (50) yields

$$\dot{V}_i \leq -3k_{1i}^{\frac{1}{3}}(\bar{\Omega}_{\alpha i}\Omega_{\alpha i})^{-\frac{2}{3}}\eta_{\alpha i}^2 - 2k_{2i}^{\frac{1}{2}}\eta_{\alpha i}^2 - \tilde{v}_{0i}^TG_i\tilde{v}_{0i} + \bar{C}_i$$

where $\bar{C}_i = C_i + 3$. Thus, we obtain $\dot{V}_i \leq -\mu_i V_i + \bar{C}_i$ from (48), where $\mu_i = \min\{6k_{1i}^{\frac{1}{3}}(\bar{\Omega}_{\rho i}\underline{\Omega}_{\rho i})^{-\frac{2}{3}}, 4k_{2i}^{\frac{1}{2}}, 2\frac{\lambda_{\min}(G_i)}{\lambda_{\max}(\Gamma_{0i}^{-1})}\}$, which implies that

$$V_i(t) \le \left(V_i(0) - \frac{\bar{C}_i}{\mu_i}\right) e^{-\mu_i t} + \frac{\bar{C}_i}{\mu_i}.$$

From (48), when $t\to\infty$, we obtain $\frac{1}{2}\eta_{\rho i}^2\leq\frac{\bar{C}_i}{\mu_i}$ and $\frac{1}{2}\tilde{v}_{0i}^T\Gamma_{0i}^{-1}\tilde{v}_{0i}\leq\frac{\bar{C}_i}{\mu_i}$, which produces

$$|\eta_{\rho i}| \leq \sqrt{\frac{2\bar{C}_i}{\mu_i}}, \ ||\tilde{v}_{0i}|| \leq \sqrt{\frac{2\bar{C}_i}{\mu_i \lambda_{\min}(\Gamma_{0i}^{-1})}}.$$

Similar to Theorem 1(iii), small \bar{C}_i and large μ_i are preferred by selecting large gains k_{1i} and Γ_{0i} such that the relative distance error $e_{\rho i}(t)$ and the estimation error $\tilde{v}_{0i}(t)$ will converge to small neighborhoods of the origin when $\rho_i^*(t) \geq R_{ci}$.

(iv) Consider the following Lyapunov function candidate

$$V_{\alpha i} = \frac{1}{2} \eta_{\alpha i}^2 \tag{52}$$

whose derivative along (2), (12), (24), (29), and the control law (26) yields

$$\dot{V}_{\alpha i} = -k_{2i} \bar{\Omega}_{\alpha i} \underline{\Omega}_{\alpha i} \frac{\partial \eta_{\alpha i}}{\partial e_{\alpha i}} \eta_{\alpha i}^{2} + \eta_{\alpha i} \frac{\partial \eta_{\alpha i}}{\partial e_{\alpha i}} \frac{\bar{\varphi}_{i}^{T} \tilde{v}_{0i}}{\rho_{i}} \\
- \left(\frac{\eta_{\alpha i}}{\rho_{i}} \frac{\partial \eta_{\alpha i}}{\partial e_{\alpha i}}\right)^{2} - \left(\eta_{\alpha i} \frac{\partial \eta_{\alpha i}}{\partial e_{\alpha i}}\right)^{2} - \eta_{\alpha i} \frac{\partial \eta_{\alpha i}}{\partial e_{\alpha i}} \dot{\phi}_{i_{+}}. (53)$$

According to (43)–(45), it is clear that (53) leads to

$$\dot{V}_{\alpha i} \le -k_{2i} \eta_{\alpha i}^4 + \frac{1}{2\epsilon_{\alpha i}^2} \tilde{v}_{0i}^T \tilde{v}_{0i} + \frac{1}{2\epsilon_{\alpha \alpha}^2} \dot{\phi}_{i_+}^2 \tag{54}$$

with $\frac{\epsilon_{\alpha_1}^2}{2} < 1$ and $\frac{\epsilon_{\alpha_2}^2}{2} < 1$. Theorem 2(i) and Theorem 1(ii), respectively, show the boundedness of \tilde{v}_{0i} and $\dot{\phi}_{i_+}$, i.e., $||\tilde{v}_{0i}|| \leq \varrho_4$ and $|\dot{\phi}_{i_+}| \leq c_{i_+}$, which implies that (54) leads to

$$\dot{V}_{\alpha i} \le -k_{2i} \eta_{\alpha i}^4 + C_{\alpha i} \tag{55}$$

where $C_{\alpha i}=\frac{1}{2\epsilon_{\alpha_1}^2}\varrho_4^2+\frac{1}{2\epsilon_{\alpha_2}^2}c_{i_+}^2$. As a result, it is from (51), (52), and (55) that $\dot{V}_{\alpha i}\leq -\mu_{\alpha i}V_{\alpha i}+\bar{C}_{\alpha i}$, where $\mu_{\alpha i}=4k_{2i}^{\frac{1}{2}}$ and $\bar{C}_{\alpha i}=C_{\alpha i}+1$, which implies that

$$V_{\alpha i}(t) \le \left(V_{\alpha i}(0) - \frac{\bar{C}_{\alpha i}}{\mu_{\alpha i}}\right) e^{-\mu_{\alpha i} t} + \frac{\bar{C}_{\alpha i}}{\mu_{\alpha i}}.$$

It follows from (52) that as $t \to \infty$, we obtain that $\frac{1}{2}\eta_{\alpha i}^2 \le \frac{\bar{C}_{\alpha i}}{\mu_{\alpha i}}$, which yields $|\eta_{\alpha i}| \le \sqrt{\frac{2\bar{C}_{\alpha i}}{\mu_{\alpha i}}}$. Similar to Theorem 1(iii), to ensure the convergence set $\{e_{\alpha i}: -\underline{\Lambda}_{\alpha i} \le e_{\alpha i} \le \bar{\Lambda}_{\alpha i}$, as $t \to \infty\}$ being small as possible, small $\bar{C}_{\alpha i}$ and large $\mu_{\alpha i}$ are desirable by selecting a large gain k_{2i} . Therefore, the angle error $e_{\alpha i}(t)$ will converge to a small neighbourhood of zero with or without obstacles.

REFERENCES

- H. Yamaguchi, "A cooperative hunting behavior by mobile-robot troops," *The International Journal of Robotics Research*, vol. 18, no. 9, pp. 931– 940, 1999.
- [2] T.-H. Kim and T. Sugie, "Cooperative control for target-capturing task based on a cyclic pursuit strategy," *Automatica*, vol. 43, no. 8, pp. 1426– 1431, 2007.
- [3] N. Ceccarelli, M. Di Marco, A. Garulli, and A. Giannitrapani, "Collective circular motion of multi-vehicle systems," *Automatica*, vol. 44, no. 12, pp. 3025–3035, 2008.
- [4] Y. Lan, G. Yan, and Z. Lin, "Distributed control of cooperative target enclosing based on reachability and invariance analysis," *Systems & Control Letters*, vol. 59, no. 7, pp. 381–389, 2010.
- [5] R. Zheng, Y. Liu, and D. Sun, "Enclosing a target by nonholonomic mobile robots with bearing-only measurements," *Automatica*, vol. 53, pp. 400–407, 2015.
- [6] R. Li, Y. Shi, and Y. Song, "Localization and circumnavigation of multiple agents along an unknown target based on bearing-only measurement: A three dimensional solution," *Automatica*, vol. 94, pp. 18–25, 2018.
- [7] X. Yu, J. Ma, N. Ding, and A. Zhang, "Cooperative target enclosing control of multiple mobile robots subject to input disturbances," *IEEE Transactions on Systems, Man, and Cybernetics: Systems*, vol. 51, no. 6, pp. 3440–3449, 2021.
- [8] M. Deghat, I. Shames, B. D. O. Anderson, and C. Yu, "Localization and circumnavigation of a slowly moving target using bearing measurements," *IEEE Transactions on Automatic Control*, vol. 59, no. 8, pp. 2182–2188, 2014.
- [9] Y. Jiang, Z. Peng, D. Wang, and C. L. P. Chen, "Line-of-sight target enclosing of an underactuated autonomous surface vehicle with experiment results," *IEEE Transactions on Industrial Informatics*, vol. 16, no. 2, pp. 832–841, 2020.
- [10] X. Peng, K. Guo, X. Li, and Z. Geng, "Cooperative moving-target enclosing control for multiple nonholonomic vehicles using feedback linearization approach," *IEEE Transactions on Systems, Man, and Cy*bernetics: Systems, vol. 51, no. 8, pp. 4929–4935, 2021.
- [11] X. Liang, H. Wang, Y.-H. Liu, W. Chen, and T. Liu, "Formation control of nonholonomic mobile robots without position and velocity measurements," *IEEE Transactions on Robotics*, vol. 34, no. 2, pp. 434– 446, 2018.
- [12] L. Dou, X. Yu, L. Liu, X. Wang, and G. Feng, "Moving-target enclosing control for mobile agents with collision avoidance," *IEEE Transactions* on Control of Network Systems, vol. 8, no. 4, pp. 1669–1679, 2021.
- [13] J. Guo, G. Yan, and Z. Lin, "Local control strategy for moving-target-enclosing under dynamically changing network topology," *Systems & Control Letters*, vol. 59, no. 10, pp. 654–661, 2010.
- [14] X. Yu and L. Liu, "Cooperative control for moving-target circular formation of nonholonomic vehicles," *IEEE Transactions on Automatic Control*, vol. 62, no. 7, pp. 3448–3454, 2017.
- [15] L. Dou, C. Song, X. Wang, L. Liu, and G. Feng, "Target localization and enclosing control for networked mobile agents with bearing measurements," *Automatica*, vol. 118, Article 109022, 2020.
- [16] X. Yu, X. Xu, L. Liu, and G. Feng, "Circular formation of networked dynamic unicycles by a distributed dynamic control law," *Automatica*, vol. 89, pp. 1–7, 2018.

- [17] G. López-Nicolás, M. Aranda, and Y. Mezouar, "Adaptive multirobot formation planning to enclose and track a target with motion and visibility constraints," *IEEE Transactions on Robotics*, vol. 36, no. 1, pp. 142–156, 2020.
- [18] S. Ju, J. Wang, and L. Dou, "Enclosing control for multiagent systems with a moving target of unknown bounded velocity," *IEEE Transactions* on Cybernetics, vol. 52, no. 11, pp. 11561–11570, 2022.
- [19] C. K. Verginis, A. Nikou, and D. V. Dimarogonas, "Robust formation control in SE(3) for tree-graph structures with prescribed transient and steady state performance," *Automatica*, vol. 103, pp. 538–548, 2019.
- [20] S.-L. Dai, K. Lu, and J. Fu, "Adaptive finite-time tracking control of nonholonomic multirobot formation systems with limited field-of-view sensors," *IEEE Transactions on Cybernetics*, vol. 52, no. 10, pp. 10695– 10708, 2022.
- [21] C. Wang and G. Xie, "Limit-cycle-based decoupled design of circle formation control with collision avoidance for anonymous agents in a plane," *IEEE Transactions on Automatic Control*, vol. 62, no. 12, pp. 6560–6567, 2017.
- [22] C. Wang, W. Xia, and G. Xie, "Limit-cycle-based design of formation control for mobile agents," *IEEE Transactions on Automatic Control*, vol. 65, no. 8, pp. 3530–3543, 2020.
- [23] Z. Yang, C. Chen, S. Zhu, X. Guan, and G. Feng, "Distributed entrapping control of multiagent systems using bearing measurements," *IEEE Transactions on Automatic Control*, vol. 66, no. 12, pp. 5696–5710, 2021.
- [24] K. P. Tee, S. S. Ge, and E. H. Tay, "Barrier Lyapunov functions for the control of output-constrained nonlinear systems," *Automatica*, vol. 45, no. 4, pp. 918–927, 2009.
- [25] K. Zhao, Y. Song, and Z. Zhang, "Tracking control of MIMO nonlinear systems under full state constraints: A single-parameter adaptation approach free from feasibility conditions," *Automatica*, vol. 107, no. 107, pp. 52–60, 2019.
- [26] X. Jin, "Adaptive fixed-time control for MIMO nonlinear systems with asymmetric output constraints using universal barrier functions," *IEEE Transactions on Automatic Control*, vol. 64, no. 7, pp. 3046–3053, 2019.
- [27] F. Chen and D. V. Dimarogonas, "Leader-follower formation control with prescribed performance guarantees," *IEEE Transactions on Control* of Network Systems, vol. 8, no. 1, pp. 450–461, 2021.
- [28] X. Jin, "Fault tolerant finite-time leader-follower formation control for autonomous surface vessels with LOS range and angle constraints," *Automatica*, vol. 68, pp. 228–236, 2016.
 [29] C. K. Verginis, C. P. Bechlioulis, D. V. Dimarogonas, and K. J.
- [29] C. K. Verginis, C. P. Bechlioulis, D. V. Dimarogonas, and K. J. Kyriakopoulos, "Robust distributed control protocols for large vehicular platoons with prescribed transient and steady-state performance," *IEEE Transactions on Control Systems Technology*, vol. 26, no. 1, pp. 299–304, 2018.
- [30] F. Mehdifar, C. P. Bechlioulis, F. Hashemzadeh, and M. Baradarannia, "Prescribed performance distance-based formation control of multi-agent systems," *Automatica*, vol. 119, Article 109086, 2020.
- [31] J. Fu, Y. Lv, G. Wen, and X. Yu, "Local measurement based formation navigation of nonholonomic robots with globally bounded inputs and collision avoidance," *IEEE Transactions on Network Science and Engineering*, vol. 8, no. 3, pp. 2342–2354, 2021.
- [32] S.-L. Dai, K. Lu, and X. Jin, "Fixed-time formation control of unicycle-type mobile robots with visibility and performance constraints," *IEEE Transactions on Industrial Electronics*, vol. 68, no. 12, pp. 12615–12625, 2021.
- [33] S. Mastellone, D. M. Stipanović, C. R. Graunke, K. A. Intlekofer, and M. W. Spong, "Formation control and collision avoidance for multi-agent non-holonomic systems: Theory and experiments," *The International Journal of Robotics Research*, vol. 27, no. 1, pp. 107–126, 2008.
- [34] H. Yang, X. Fan, P. Shi, and C. Hua, "Nonlinear control for tracking and obstacle avoidance of a wheeled mobile robot with nonholonomic constraint," *IEEE Transactions on Control Systems Technology*, vol. 24, no. 2, pp. 741–746, 2016.
- [35] Y. Wang, M. Shan, Y. Yue, and D. Wang, "Vision-based flexible leader-follower formation tracking of multiple nonholonomic mobile robots in unknown obstacle environments," *IEEE Transactions on Control Systems Technology*, vol. 28, no. 3, pp. 1025–1033, 2020.
- [36] A. S. Lafmejani, H. Farivarnejad, and S. Berman, "Adaptation of gradient-based navigation control for holonomic robots to nonholonomic robots," *IEEE Robotics and Automation Letters*, vol. 6, no. 1, pp. 191– 198, 2021.
- [37] S. G. Loizou, D. G. Lui, A. Petrillo, and S. Santini, "Connectivity preserving formation stabilization in an obstacle-cluttered environment in

the presence of time-varying communication delays," *IEEE Transactions on Automatic Control*, vol. 67, no. 10, pp. 5525–5532, 2022.



Ke Lu received the B.E. degree in material engineering from Nanjing Forestry University, Nanjing, China, in 2015, and the M.Sc. degree in mechanical and automation engineering from the Chinese University of Hong Kong, Hong Kong, in 2017. He is currently pursuing the Ph.D. degree in control science and engineering with the School of Automation Science and Engineering, South China University of Technology, Guangzhou, China.

His current research interests include adaptive control system, coordination and control of multi-agent systems.



Shi-Lu Dai (S'09–M'11) received his B.Eng. degree in thermal engineering in 2002, and his M.Eng. and Ph.D. degrees in control science and engineering in 2006 and 2010, respectively, from the Northeastern University, Shenyang, China.

He was a Visiting Student in the Department of Electrical and Computer Engineering, National University of Singapore, Singapore, from November 2007 to November 2009, and a Visiting Scholar at the Department of Electrical Engineering, University of Notre Dame, Notre Dame,

IN, USA, from October 2015 to October 2016. Since 2010, he has been with the School of Automation Science and Engineering, South China University of Technology, Guangzhou, China, where he is currently a Professor. His current research interests include adaptive and learning control, distributed cooperative systems.



Xu Jin (S'12–M'19) received the Bachelor of Engineering (BEng) degree in electrical and computer engineering (First Hons.) from the National University of Singapore, Singapore, in 2013, the Master of Applied Science (MASc) degree in electrical and computer engineering from the University of Toronto, Toronto, ON, Canada, in 2015, the Master of Science (MS) degree in mathematics from the Georgia Institute of Technology, Atlanta, GA, USA, in 2018, and the Doctor of Philosophy (PhD) degree in aerospace

engineering from the Georgia Institute of Technology, Atlanta, GA, USA, in 2019.

Dr. Jin is currently an Assistant Professor with the Department of Mechanical and Aerospace Engineering, University of Kentucky, Lexington, KY, USA. He has authored/co-authored over 50 peer-reviewed journal and conference papers. He has been a reviewer for over 20 journals in areas of control systems and applications. His current research interests include adaptive and iterative learning control, fault-tolerant control, nonlinear systems control, with applications to intelligent vehicles, autonomous robots, and multiagent systems.